# QUANTUM RANDOM WALK SIMULATION USING DEPENDENT RANDOM WALK

A THESIS SUBMITTED TO
THE GRADUATE SCHOOL OF NATURAL AND APPLIED SCIENCES
OF
MIDDLE EAST TECHNICAL UNIVERSITY

BY

MERT KAŞIF CEYLAN

IN PARTIAL FULFILLMENT OF THE REQUIREMENTS
FOR
THE DEGREE OF MASTER OF SCIENCE
IN
STATISTICS

SEPTEMBER 2024

Approval of the thesis:

**QUANTUM RANDOM WALK SIMULATION USING DEPENDENT RANDOM WALK**

submitted by **MERT KAŞIF CEYLAN** in partial fulfillment of the requirements for the degree of **Master of Science in Statistics Department, Middle East Technical University** by,

Prof. Dr. Naci Emre Altun
Dean, Graduate School of **Natural and Applied Sciences** _____

Prof. Dr. Ayşen Dener Akkaya
Head of Department, **Statistics** _____

Assoc. Prof. Dr. Ceren Vardar Acar
Supervisor, **Statistics, METU** _____

**Examining Committee Members:**

Prof. Dr. Vilda Purutçuoğlu
Statistics, METU _____

Assoc. Prof. Dr. Ceren Vardar Acar
Statistics, METU _____

Assoc. Prof. Dr. Yakup Murat Bulut
Statistics, Eskisehir Osmangazi University _____

Date:06.09.2024

**I hereby declare that all information in this document has been obtained and presented in accordance with academic rules and ethical conduct. I also declare that, as required by these rules and conduct, I have fully cited and referenced all material and results that are not original to this work.**

Name, Surname: Mert Kaşif Ceylan

Signature :

# ABSTRACT

## QUANTUM RANDOM WALK SIMULATION USING DEPENDENT RANDOM WALK

Ceylan, Mert Kaşif
M.S., Department of Statistics
Supervisor: Assoc. Prof. Dr. Ceren Vardar Acar

September 2024, 59 pages

Quantum computers have sparked significant interest in recent years due to their potential to revolutionize various fields. One area where quantum computing shows great promise is in the study of quantum walks, a quantum counterpart of the classical random walk algorithm that has been foundational in scientific research. While both quantum and classical random walks involve a "walker" moving through a space or graph, quantum walks differ fundamentally due to quantum principles such as superposition, leading to unique behaviors like linear spreading and localization.

This thesis investigates the quantum walk simulation, with a particular focus on the Quantum-Walk-Replicating-Random-Walk (QWRW) model. Unlike traditional quantum walks, which sum over all possible paths with complex interference effects, the QWRW approach models the walk as a series of distinct, classical-like steps. This trajectory-based perspective offers a novel way to analyze the walker's position and movement, avoiding the complexities of quantum interference.

The QWRW model is particularly valuable in understanding key phenomena of quantum walks, such as linear spreading and localization, by providing insights into the

directional properties of quantum walkers. By defining transition probabilities in both space and time, the QWRW model offers a detailed framework for examining the spatial and temporal characteristics of quantum walks, enhancing our understanding of their behavior and potential applications. This study aims to bridge the gap between classical and quantum walks, contributing to the broader field of quantum computing and its practical implications.

Keywords: Quantum, Random Walk, Quantum Random Walk, Simulation

# ÖZ

## BAĞIMLI RASTGELE YÜRÜYÜŞ KULLANILARAK KUANTUM RASTGELE YÜRÜYÜŞ SİMÜLASYONU

Ceylan, Mert Kaşif
Yüksek Lisans, İstatistik Bölümü
Tez Yöneticisi: Doç. Dr. Ceren Vardar Acar

Eylül 2024 , 59 sayfa

Kuantum bilgisayarlar, çeşitli alanlarda devrim yaratma potansiyelleri nedeniyle son yıllarda büyük ilgi uyandırmıştır. Kuantum bilişimin umut vaat ettiği alanlardan biri, bilimsel araştırmalarda temel bir rol oynayan klasik rastgele yürüyüş algoritmasının kuantum karşılığı olan kuantum yürüyüşleridir. Hem kuantum hem de klasik rastgele yürüyüşler, bir "yürüyüşçünün" bir alan veya grafik üzerinde hareket etmesini içerirken, kuantum yürüyüşler süperpozisyon gibi kuantum ilkeleri nedeniyle temel olarak farklılık gösterir ve bu da lineer yayılma ve yerelleşme gibi benzersiz davranışlara yol açar.

Bu tez, Kuantum-Yürüyüş-Replikasyonlu-Rastgele-Yürüyüş (QWRW) modeli üzerinde odaklanarak kuantum yürüyüş simülasyonunu incelemektedir. Geleneksel kuantum yürüyüşlerinin karmaşık girişim etkileriyle tüm olası yolları toplamasının aksine, QWRW yaklaşımı yürüyüşü, belirgin ve klasik benzeri adımlar dizisi olarak modellemektedir. Bu yörünge temelli bakış açısı, yürüyüşçünün pozisyonunu ve hareketini analiz etmek için yenilikçi bir yol sunar, kuantum girişiminin karmaşıklıklarını ortadan kaldırır.

QWRW modeli, kuantum yürüyüşlerin yönsel özellikleri hakkında içgörüler sunarak lineer yayılma ve yerelleşme gibi kuantum yürüyüşlerin kilit fenomenlerini anlamada özellikle değerlidir. Hem uzayda hem de zamanda geçiş olasılıklarını tanımlayarak, QWRW modeli kuantum yürüyüşlerin mekansal ve zamansal özelliklerini incelemek için ayrıntılı bir çerçeve sunar ve davranışlarını ve olası uygulamalarını daha iyi anlamamızı sağlar. Bu çalışma, klasik ve kuantum yürüyüşler arasındaki boşluğu doldurmayı amaçlayarak, kuantum bilişim alanına ve pratik yansımalarına katkıda bulunmaktadır.

Anahtar Kelimeler: Kuantum, Rastgele Yürüyüş, Kuantum Rasgele Yürüyüş, Benzetim

To my family, whose unwavering love and support have been my foundation, and to my friends, whose encouragement and belief in me have guided me through this journey.

## ACKNOWLEDGMENTS

I would like to extend my deepest gratitude to my thesis supervisor, Assoc. Prof. Dr. Ceren Vardar Acar, for her invaluable guidance, support, and dedication. Despite working on this topic with me for the first time, her unwavering determination was nothing short of inspiring. Her patience, understanding, and constant encouragement have been crucial to the completion of this thesis. I feel incredibly fortunate to have had her as my mentor and am deeply grateful for her insights and tireless efforts.

I would like to thank Assoc. Prof. Dr. Yakup Murat Bulut for introducing me to the field of statistics and fostering my passion for this area. His support has been a great source of motivation, and meeting him was a true turning point in my life.

I am also grateful to Assoc. Prof. Dr. Fulya Gökalp Yavuz for providing me with a scholarship through her project and for her support during this process.

Special thanks to my classmates Mehmet Bi, Berk Akyüz, Hilal Erdeniz, Yeşim Koçoğlu, and Bengisu Açıkgöz. Throughout this journey, we shared a great synergy, always supporting and encouraging each other, which made navigating the challenges of this academic process much easier.

I would also like to express my gratitude to the department assistants Rana Arslan, İrem Tanrıverdi, Serenay Çakar, Petek Aydemir for their friendship and helpfulness throughout this journey.

Lastly, to my dear friends Bahadır Çamcıoğlu, Çağrı Köşe, Enes Tekelli, Halit Bayrak, Kıvanç Çakıroğlu, Murat Yaman, and Veysel Baltak, I am deeply thankful for your constant moral support and encouragement.

## TABLE OF CONTENTS

ABSTRACT . . . . . v

ÖZ . . . . . vii

ACKNOWLEDGMENTS . . . . . x

TABLE OF CONTENTS . . . . . xi

LIST OF FIGURES . . . . . xiii

LIST OF ABBREVIATIONS . . . . . xv

CHAPTERS

1 INTRODUCTION . . . . . 1

1.1 Quantum Random Walk . . . . . 1

1.2 Classical Random Walk . . . . . 3

1.3 One Dimensional Quantum Random Walk . . . . . 4

1.4 Motivation and Problem Definition . . . . . 5

1.5 The Outline of the Thesis . . . . . 7

2 CLASSICAL RANDOM WALK . . . . . 9

2.1 Simple Random Walk . . . . . 9

2.2 Expectation . . . . . 12

2.3 The Variance . . . . . 13

3 QUANTUM WALK . . . . . 17

3.1 Quantum Walk . . . . . 17

4 SIMULATION . . . . . 33

4.1 Computations Regarding Quantum Walk . . . . . 33

4.2 Simulation of Quantum Walk . . . . . 40

5 LONGEST HEAD RUN IN QUANTUM RANDOM WALK . . . . . 49

5.1 Quantum Walk Implementation . . . . . 52

6 CONCLUSION . . . . . 55

REFERENCES . . . . . 57

## LIST OF FIGURES

FIGURES

Figure 2.1 The distribution of a RW after $t = 100$ steps is illustrated, with the probability of a rightward step being $p_r = \frac{1}{2}$. The distribution shows that the probability mass points with zero mass are evenly distributed along the $x$-axis at odd values of $x$. This is because the walker always lands on even or odd $x$-values depending on whether N is even or odd. Since $t = 100$ is even, the chance of the walker ending up on an odd $x$-value is exactly zero. . . . . 11

Figure 3.1 Chance of finding the walker at position $n$ at time $t$, starting from origin with coin in "heads" state and without any intermediate measurements, can be determined. This involves applying the operator $U$ once. The operator $U$ is repeatedly applied without making any measurements in between. At a specific time $t$, the state describes the distribution of position of particle. . . . . 23

Figure 3.2 Frequency plot for initial condition $|\psi(0)\rangle = |1\rangle|n = 0\rangle$. [21] . . 29

Figure 3.3 Frequency plot after 100 steps for symmetric QW. [21] . . . . . 30

Figure 4.1 Left and right probabilities for 5 time step iterated QWRW, [26] . 43

Figure 4.2 Probability distribution $\nu_n(x)$ of the QWRW at time $n = 500$, [26] 44

Figure 4.3 100 simulated paths for $n = 500$, [26] . . . . . 45

Figure 4.4 Sample path generated with provided MATLAB code for $n = 500$ . . . . . 47

Figure 5.1 Values of $C_n^{(k)}(3)$ for $n \leq 8$ . . . . . 52

## LIST OF ABBREVIATIONS

ABBREVIATIONS

All the distributions should be understood as probability distribution

RW = Random Walk

QW = Quantum (Random) Walk

QWRW = Quantum Walk Random Walk

HS = Hilbert Space

# CHAPTER 1

# INTRODUCTION

## 1.1 Quantum Random Walk

Quantum mechanics explains the behavior of matter and energy in terms of superposition and entanglement. It serves as the fundamental basis for different branches of physics, especially in quantum information science and quantum chemistry [10]. While classical physics effectively describes numerous aspects of nature at both everyday macroscopic and microscopic scales, it falls short at the extremely small submicroscopic (atomic and subatomic) levels. Quantum mechanics, however, can account for these small-scale phenomena. Many classical physics theories can be derived as approximations of this phenomenon, valid at larger (macroscopic/microscopic) scales [12]. Quantum computers leverage superposition and entanglement principles in quantum mechanics to create states that expand exponentially with increase in number of qubits (quantum bits), [1]. Superposition is a key principle in quantum physics, where a quantum system can simultaneously exist in several states until it is measured. Unlike classical mechanics where a particle occupies a definite state, a quantum particle can be described by a wave function representing a distribution across various possible states and entanglement is a quantum phenomenon where two or more particles become interconnected, regardless of distance separating them. This means that the state of one particle instantaneously influences state of the other, a correlation that defies classical physics. Classical computers have been utilized extensively over many years and have made substantial contributions to scientific progress. On the other hand, quantum computing has shown promise in addressing extensive and intricate problems [5]. Integrating principles from quantum mechanics with classical random walks introduces a new paradigm: quantum walks.

Quantum walk first introduced by Aharanov [3], which established the groundwork for a theory of quantum walks on graphs, which generalizes random walks on finite graphs to quantum domain. This theory was first proposed by them. These quantum walks possess remarkable computational capabilities and find extensive applications across many fields, [13]. For instance, In cryptology, a new double medical image encryption algorithm designed to address potential vulnerabilities in medical image cryptosystems due to advancement of quantum random walks [2]. Their technique involves splitting each medical image into two separate images: one containing the high 4 bits of each pixel, and the other containing the low 4 bits. The high-bit image, which carries most of the information, is encrypted using quantum walks, while the low-bit image, which carries less information, is encrypted using logistic mapping. The effectiveness of this encryption method is demonstrated and results indicate the proposed technique's efficiency in securely encrypting medical images. In engineering domain, in the study of [24], a quantum walk framework was developed for one- and two-dimensional spaces where potentials affect the quantum walker's "charge," with the walk's evolution influenced by both constant and time-varying potentials. In their work, they reproduce phenomena like tunneling through a barrier and analyze the quantum walk's behavior in spaces with different potential distributions. It is demonstrated that practical applications by using their model to simulate maze navigation and vehicle movement in urban environments, where curbs and buildings are represented as impenetrable potential barriers and traffic lights as time-varying potential barriers. This formulation suggests that quantum walks in potential-applied spaces can be a foundation for applied quantum computing, potentially leading to new quantum algorithms where inputs are introduced as potential profiles. Another study in computer science [9], quantum walk used to explore new quantum algorithms that have potential to outperform classical computation in manner of complexity. Instead of focusing on the well-known non-Abelian hidden subgroup problem, they extend Shor factoring algorithm's solution by proposing a different approach: detecting hidden nonlinear structures over finite fields. They provide two instances of such issues that quantum computers can efficiently solve, unlike classical computers. Additionally, promising results were provided about quantum query complexity associated with the detection of these hidden nonlinear structures. İt is shown that quantum algorithms can significantly outperform classical algorithms in this domain.

Lastly in biology, Irwin Huang and Yu-Ping Huang [11] address the challenge of decoherence and disorder in quantum systems, which typically hinder their performance in practical applications. The potential for these two factors to counteract each other was explored, thereby preserving some of the systems' quantum characteristics. The optimal level of disorder that mitigates effects of decoherence in one- and two-dimensional quantum random walks was explored. This approach significantly increases the mean walking distance across various decoherence strengths, indicating a promising strategy for developing practical quantum systems that are resilient to both decoherence and disorder. Based on principles of quantum mechanics, quantum random walk emerges as a potential tool to address uncertainties and complexities in financial markets. Quantum walk may offer an approach beyond traditional methods to solve financial problems such as portfolio optimization and derivatives pricing [18].

## 1.2 Classical Random Walk

A random walk is a stochastic process, describing a path composed of a series of random steps. This concept is useful for analyzing and simulating randomness of objects and calculating correlations among them, making it valuable for practical problem-solving across many fields [25]. Random walk term was first introduced by Karl Pearson in 1905 [20]. Spitzer [19] provides a thorough review of random walks for mathematical researchers, clearly explaining the fundamental principles behind them. Random walks are also, commonly used in computer science to approximate the size of World Wide Web, [5].

In financial economics, random walk serves as a fundamental framework for modeling various aspects, including share prices. However, empirical investigations have uncovered deviations from this theoretical model, particularly regarding short-term and long-term correlations. These findings suggest that while random walk hypothesis provides a valuable starting point, it may not fully capture complexities of real-world financial dynamics [15]. Random walks are used in physics as simplified models for phenomena such as Brownian motion and diffusion. These models illustrate random movement of molecules in liquids and gases. In quantum field theory, ran-

dom walks and specific self-interacting walks hold great importance [4]. A Simple random walk model in mathematics refers to the movement of a point on a regular lattice. At each step, the point moves to a new place depending on a distribution. Quantum walks, which are analogous to classical random walks in quantum mechanics, primarily vary in their lack of convergence to limiting distributions [3]. Quantum walks have the ability to spread at significantly different speeds compared to classical walks, according to the phenomenon of quantum interference. Quantum walk-based algorithms frequently demonstrate reduced time complexity and have the potential to reach exponential acceleration compared to classical algorithms [6].

### 1.3 One Dimensional Quantum Random Walk

Quantum random walks (QRWs) in one dimension represent an extension of classical random walks, introducing unique behaviors due to quantum mechanics. David A. Meyer [17] introduced the concept of one dimensional quantum walks to demonstrate the potential of quantum computing to perform certain computational tasks more efficiently than classical computing. Specifically, he wanted to show that a quantum particle automaton, described as a lattice gas formulation with left and right moving particles, could achieve faster mixing and spreading than classical random walks. This difference arises because quantum walks leverage the principles of superposition and interference, which are fundamental to quantum mechanics. Unlike classical random walks where a particle moves left or right based on a coin flip, QRWs involve a particle that not only moves on a one-dimensional lattice but also possesses an extra internal state called chirality, which can be left or right. This internal state influences the particle's movement, ensuring the process remains unitary, which is essential in quantum mechanics. A notable example is the Hadamard walk, where the chirality undergoes a Hadamard transformation at each step, followed by movement according to the new chirality state. This unitary evolution allows for quantum interference, where different paths can cancel each other out, creating a distribution markedly different from classical random walks. QRWs are not just of theoretical interest; they hold promise for developing new quantum algorithms and advancing our understanding of quantum processes, potentially offering powerful tools for the field

of quantum computing [1]. In an example study [16], the Hadamard walk, driven by a Hadamard coin, was applied to identify crucial edges in undirected complex networks. The model assigned importance scores to edges based on the observed probabilities between node pairs, allowing for effective ranking of edge significance. Experimental results demonstrated that the Hadamard walk model outperformed existing algorithms by 4.59% to 20.03% in static networks. Furthermore, the model was tested in a dynamic network scenario involving UAV swarms, where it successfully selected significant nodes. The simulations indicated that the Hadamard walk model excelled in verifying epidemic dynamics models, showcasing its potential utility in both static and dynamic network applications. In another study [7], a novel approach was used to correlate a quantum walk, influenced by a Hadamard coin, with birth and death process.

## 1.4 Motivation and Problem Definition

In contemporary technology, the potential roles of quantum computers are actively discussed and debated. The classical random walk algorithm, extensively studied and widely used across various scientific fields, has been essential in the advancement of theories and literature. In this study, we examine the combination of random walk algorithm with quantum mechanics, resulting in the quantum walk. In this thesis, the quantum walk simulation is examined. Distinct nature of quantum walks compared to classical random walks, despite being often considered their quantum counterpart. While both processes involve a walker moving through a space or graph, underlying mechanics of quantum walks differ significantly due to quantum principles such as superposition. These differences give quantum walks unique properties, leading to behaviors not observed in classical random walks. Quantum walks have been extensively studied for their unique structure, establishing them as a key area of focus in both theoretical and applied research [26]. The quantum walk demonstrate flexible nature that varies based on the specific time and space conditions or settings.

In quantum walks, linear spreading and localization are two fundamental phenomena that distinguish them from classical random walks. Linear spreading refers to the rapid expansion of the distribution over time, with the standard deviation of walker's

position increasing proportionally to time, contrasting with slower $\sqrt{t}$ spread characteristic of classical walks. This accelerated spreading arises from quantum superposition and interference. In contrast, localization describes the phenomenon where quantum walker remains confined to a specific region of the space, despite the passage of time. Alternatively, various modified versions of classical random walks are commonly explored, such as correlated random walks [22] and Lévy walks [8]. In a Simple random walk, as number of steps increases, the distribution of walker's position tends to resemble a normal (Gaussian) distribution due to the Central Limit Theorem. This predictable pattern is useful for modeling certain types of random processes. However, when dealing with modified random walks, such as correlated random walks or Lévy walks, the distribution of the walker's position does not necessarily follow a normal distribution. These modifications introduce dependencies between steps or allow for step sizes that deviate from the usual, leading to more complex and varied distributions. This complexity is why researchers across various fields find modified random walks valuable as they can better capture and describe the intricate transitions and behaviors seen in real-world phenomena, where simple assumptions of a normal distribution may not apply.

Our main objective is to simulate and analyze a quantum walk using its trajectories, similar to a random walk. The introduction of quantum-walk-replicating-random-walk (QWRW) [26] aligns perfectly with this purpose. In traditional quantum walks, finding the walker's probability at a specific position is determined by summing up all possible paths the walker could have taken, taking into account the phase or coherence of each path. This coherent sum means that probability amplitudes (complex numbers representing both the likelihood and phase of each path) can interfere with each other, leading to constructive or destructive interference. As a result, the overall distribution is influenced by quantum interference effects of all possible paths.

In contrast, a quantum-walk-replicating-random-walk (QWRW) approach focuses on individual trajectories or paths that the walker might take to reach a position, similar to how paths are treated in classical random walks. Instead of summing over all possible paths, QWRW models walk as a series of distinct steps, each with its own probability, leading to a more classical-like understanding of the walker's movement. This approach avoids complex interference effects seen in conventional quantum walks,

providing a more straightforward, trajectory-based way to analyze the walker's position.

Instead of using coherent summation, quantum-walk-replicating-random-walk (QWRW) calculates walker's probability being at a particular position by analyzing the statistical behavior of individual walkers over time. This transforms the problem into one of transition probabilities, focusing on how walkers move step-by-step through space, which reveals the characteristic directionality of their movement.

While previous studies have explored classical analogs of quantum walks, the literature has not extensively examined how linear spreading and localization in quantum walks might be understood from this trajectory-based perspective. The quantum-walk-replicating-random-walk (QWRW) approach offers a unique advantage: it tracks the trajectory of each individual walker, providing new insights into the directivity of quantum walks.

Specifically, quantum-walk-replicating-random-walk (QWRW) model helps to analyze how future directions of quantum walkers are determined, shedding light on effects of linear spreading and localization in a novel way. Additionally, since quantum-walk-replicating-random-walk (QWRW) defines transition probabilities in both space and time, it provides a detailed framework for studying spatial and temporal characteristics of quantum walks, offering deeper understanding into their behavior and properties.

## 1.5 The Outline of the Thesis

This thesis is organized as follows: Chapter 1 provides an introduction, starting with an overview of quantum random walks, a fundamental concept in quantum computing and physics, followed by a review of classical random walks, which serve as the basis for understanding the quantum variant. The chapter continues with a discussion of one-dimensional quantum random walks, focusing on their unique properties and applications. It concludes with the motivation behind the study and a clear definition of the problem, along with an outline of thesis structure. Chapter 2 delves into classical random walks, beginning with the Simple random walk model, which is essential

for understanding the behavior of particles in a probabilistic framework. This chapter also covers the expectation and variance of random walks, providing a detailed analysis of these statistical measures and their implications. Chapter 3 shifts focus to quantum random walks, offering a comprehensive examination of this quantum phenomenon. This chapter explores mathematical underpinnings and distinctive features of quantum random walks, contrasting them with their classical counterparts to highlight their significance in various applications. Chapter 4 is dedicated to simulation, where practical aspects of the study are explored. It begins with computations related to quantum walks, detailing algorithms and numerical methods used. The chapter then presents the simulation of quantum walks, discussing results and their relevance to the research questions posed. Finally, Chapter 5 concludes the thesis, summarizing key findings, discussing their broader implications, and suggesting potential avenues for future research. This chapter provides a reflection on study's contributions to the field and its limitations.

# CHAPTER 2

# CLASSICAL RANDOM WALK

## 2.1 Simple Random Walk

Determining the position of a walker's distribution in space after a given number of step is the purpose of modelling a RW. The probability mass function ($Pr(x = i, t)$) indicates walker's probabilityarriving at point $x = i$ after $t^{\text{th}}$ steps.

Let us consider a walker that is originally situated at the real line's $x = 0$. To discretize this axis, define $x = il$ for a constant $l$. Then, assign integer values of $i$ to the points that the walker can access. To simplify, we will operate with a unit of length where $l = 1$. Similarly, divide the walker's motion over time into $N$ distinct time intervals by defining $t = N\tau$ by adjusting $\tau$ accordingly.

Each phase of the process begins with the toss of a coin. At each time step, the walker can go right or left. If it comes up heads, the walker moves to right, advancing from position $x = i$ to $i + 1$. If it comes up tails, the walker moves to left, going from $i$ to $i - 1$. Now, define a fixed value $p_r$ to denote walker's probability moving to right, and a constant $p_l = 1 - p_r$ denotes walker's probability moving to left. This enables the coin to be biased towards either heads or tails.

After the $t^{th}$ iteration, the walker has moved $n_l$ steps left and $n_r$ steps right, under the condition that $n_r + n_l = t$. This relationship allows for expressing $n_l$ in terms of $n_r$ and $N$.

The objective is to determine a function $Pr(i, t)$ that, after the $t$-th step, gives walker's probabilitybeing at position $x = i$. Each movement to right or left increases the overall chance that the walker will be at position $x = i$ after the $t^{th}$ step by a multiplicative

factor, $p_l = 1 - p_r$ since each step is independent. As a result, the probability that

$$p_r^{n_r} \left(1 - p_r\right)^{N - n_r} \tag{2.1}$$

the walker will end up at the location $x = i$ after taking $n_r$ rightward steps and $n_l$ leftward steps, irrespective of the sequence in which the steps are taken. The factor $p_r^{n_r}(1 - p_r)^{t - n_r}$ indicates the contribution of each unique path, which consists of $n_l$ movements to left and $n_r$ movements to right, to the overall probability of the walker reaching position $x = i$, at the $t^{th}$ step. Number of ways to choose $n_r$ rightward steps from $t$ total steps is represented by the binomial coefficient $\binom{t}{n_r}$. This calculates number of different paths that the walker can take to arrive at $x = i$. The total probability the the walker is at position $x = i$ after the $t$-th step, given that all sequences are equally likely, is given by

$$\Pr\left(R = n_r\right) = f\left(n_r\right) = \binom{t}{n_r} p_r^{n_r} \left(1 - p_r\right)^{t - n_r} \tag{2.2}$$

Let $R$ represent a random binomial variable, which represents count of steps is taken in rightward direction. The probability mass function $f(n_r)$, which aids in using computer software to display the distribution of the walker's location, has been defined.

Having a function that determines the probability of a walker arriving at $x = i$ is usually more helpful than using $n_r$ as the input for the function. To accomplish this, Equation (2.2) is expressed in terms of the walker's final position $x = i$, rather than using the number of rightward steps $R = n_r$.

To determine the walker reaching position $x = i$ probability on $i$ at $t^{\text{th}}$ step, modify Equation (2.2) by introducing a parameterization $n_r(x)$ for the variable $n_r$ and then substituting this parameterization into Equation (2.2).

To determine the expression $n_r = n_r(x)$, observe that the walker reaches position $x = n_r - n_t = 2n_r - N$ after completing $N$ steps. Rearranging this equation gives:

$$n_r = \frac{1}{2}(i + t) \tag{2.3}$$

By substituting this value into Equation (2.2), walker's probability being at position

$x = i$ is determined by following the $t^{th}$ step.

$$\text{Prob}(x = i) = \begin{cases} 0 & \text{if } \frac{1}{2}(i+t) \mod 1 \neq 0 \\ f\left(\frac{1}{2}(i+t)\right) & \text{otherwise} \end{cases} \tag{2.4}$$

The probability of $x$ being equal to $i$ is zero if the condition $\frac{1}{2}(i+t) \bmod 1 \neq 0$ is not satisfied. This constraint is crucial for visualizing the distribution as a function $\text{Prob} : \mathbb{Z} \to \mathbb{R}$, where $i \mapsto f\left(\frac{1}{2}(i+t)\right)$. If this condition is not met, it may result in a non-zero probability for positions that are half-integers.

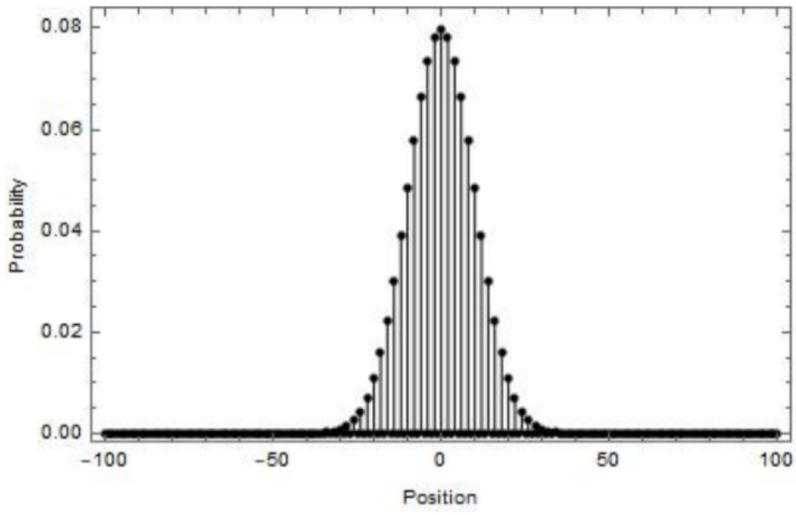



Figure 2.1: The distribution of a RW after $t = 100$ steps is illustrated, with the probability of a rightward step being $p_r = \frac{1}{2}$. The distribution shows that the probability mass points with zero mass are evenly distributed along the $x$-axis at odd values of $x$. This is because the walker always lands on even or odd $x$-values depending on whether N is even or odd. Since $t = 100$ is even, the chance of the walker ending up on an odd $x$-value is exactly zero.

To verify consistency, it can be effectively demonstrated using computational software that

$$\sum_{i=-100}^{100} \Pr(x = i, t = 100) = 1 \tag{2.5}$$

which gives the probability mass function explicitly in terms of $N$ to make it clear that the walker has taken 100 steps in total.

## 2.2 Expectation

The anticipated position of the walker following $N$ steps is given by

$$\mathbb{E}[X] = \sum_{i=-t}^{t} i \cdot \Pr(x = i) \tag{2.6}$$

The summation removes points outside the interval $[-t, t]$ since the chance of the absolute value of $x$ being greater than $t$ is zero.

By utilizing the equation $x = n_r - n_l$ and applying the principle of linearity in the calculation of the expected value,

$$\begin{aligned}
\mathbb{E}[X] &= \mu(n_r) - \mu(n_l) \\
&= \sum_{i=0}^{t} i \cdot \Pr\left(n_r = i\right) - \sum_{j=0}^{t} j \cdot \Pr\left(n_l = j\right) \\
&= \sum_{i=1}^{N} i \cdot \binom{t}{i} {p_r}^i \left(1 - p_r\right)^{t-i} - \sum_{j=1}^{t} j \cdot \binom{t}{j} {p_l}^j \left(1 - p_l\right)^{t-j}
\end{aligned} \tag{2.7}$$

The final expression is derived by incorporating Equation (2.2) into the subsequent line of Equation (2.6) and modifying the starting point of both summations from 0 to 1, since the initial term in each summation is zero. Note that in Equation (2.6), each summation is evaluated for $i$ and $j$ ranging from 0 to $t$, whereas in Equation (2.5), the summation is performed for $i$ ranging from $-t$ to $t$. This difference arises because $n_r$ and $n_l$ denote the number of steps in a single direction (right or left) along the $x$-axis, whereas $x$ accounts for the cumulative count of steps taken in both directions. By applying the first summation from Equation (2.6) and factoring out a term of $t$ from $\binom{t}{i} = \frac{t!}{i!(t-i)!}$

$$\begin{aligned}
\sum_{i=1}^{t} i \cdot \binom{t}{i} p_r^i \left(1 - p_r\right)^{t-i} &= \sum_{i=1}^{t} i \cdot \frac{t(t-1)!}{i!(t-i)!} {p_r}^i \left(1 - p_r\right)^{t-i} \\
&= t p_r \sum_{i=1}^{t-1} \frac{(t-1)!}{(i-1)![(t-1)-(i-1)]!} p_r^{i-1} \left(1 - p_r\right)^{t-i} \\
&= t p_r \sum_{i=1}^{t-1} \binom{t-1}{i-1} p_r^{i-1} \left(1 - p_r\right)^{t-i}
\end{aligned} \tag{2.8}$$

Transforming the summation on right side of the Equation (2.7) by changing $M$ to $t-1$ and $k$ to $i-1$, and then applying the binomial theorem,

$$\begin{aligned}\sum_{i=1}^{t} i \cdot \binom{t}{i} p_r^i \left(1-p_r\right)^{t-i} &= t p_r \sum_{k=0}^{M} \binom{M}{k} {p_r}^k \left(1-p_r\right)^{M-k} \\ &= t p_r \left[p_r + (1-p_r)\right]^M \\ &= t p_r\end{aligned} \tag{2.9}$$

By replacing this value in Equation (2.6) and following the same steps for the second term in Equation (2.6),

$$\mathbb{E}[X] = t\left(p_r - p_l\right) \tag{2.10}$$

is obtained. As a brief consistency check, it is crucial to note that (2.9) matches $-t, 0, t$ for the specific cases where $p_r$ equals $0$, $\frac{1}{2}$, and $1$, as expected.

## 2.3 The Variance

Finding the variance $\sigma^2 = \mathbb{E}[X^2] - \mathbb{E}[X]^2$ requires $\mathbb{E}[X^2]$,

$$\begin{aligned}\mathbb{E}[X^2] &= \mu\left(n_r - n_l\right)^2 \\ &= \mu\left(2n_r - t\right)^2 \\ &= 4\mu(n_r^2) + t^2 - 4t\mu(n_r)\end{aligned} \tag{2.11}$$

where

$$\mu(n_r^2) = \sum_{i=0}^{t} i^2 \cdot \Pr\left(n_r = i\right) \tag{2.12}$$

By substituting Equation (2.2) into Equation (2.11) and applying the same procedures as in Equation (2.7), but excluding the additional $i$ factor from the adjustments:

$$\mu(n_r^2) = t p_r \sum_{i=1}^{t-1} i \cdot \binom{t-1}{i-1} p_r^{i-1} \left(1-p_r\right)^{t-i} \tag{2.13}$$

is derived Using $M = t - 1, j = i - 1$ into (2.13) gives,

$$\begin{aligned}
\mu(n_r^2) &= tp_r \sum_{j=0}^{M} (j+1) \cdot \binom{M}{j} p_r^{\,j} \left(1 - p_r\right)^{M-j} \\
&= tp_r \sum_{j=0}^{M} (j+1) \cdot \binom{M}{j} {p_r}^{j} \left(1 - p_r\right)^{M-j} \\
&= tp_r \sum_{j=0}^{M} j \cdot \binom{M}{j} {p_r}^{j} \left(1 - p_r\right)^{M-j} + tp_r \sum_{j=0}^{M} \binom{M}{j} {p_r}^{j} \left(1 - p_r\right)^{M-j}
\end{aligned} \tag{2.14}$$

The expression on right-hand side, represented by $\sum_{j=0}^{M} \binom{M}{j} p_r^j (1 - p_r)^{M-j}$, is equal to 1, as it is necessary for the total sum of probabilities to be one. The second term in the expression is equal to the product of $N$ and $p_r$. When examining the summation in the initial phrase on right side of Equation (2.14) and comparing it to Equation (2.8), it becomes apparent that both represent the expected value of a binomial random variable with parameters $M$ and $p_r$. Consider that $M = t - 1$, the summation in the initial phrase simplifies to $(t - 1)p_r$. Thus,

$$\mu(n_r^2) = tp_r \left[(t-1)p_r + 1\right] \tag{2.15}$$

By substituting Equation (2.15) into Equation (2.10) and thereafter organizing the terms based on powers of $t$.

$$\begin{aligned}
\mathbb{E}[X^2] &= 4\left(N^2 {p_r}^2 - N{p_r}^2 + Np_r\right) + N^2 - 4N\mu(n_r) \\
&= \left(4p_r^2 - 4p_r + 1\right) N^2 + 4p_r \left(1 - p_r\right) N
\end{aligned} \tag{2.16}$$

By utilizing the equation $\langle n_r \rangle = Np_r$ to substitute terms in Equation (2.16) simply replacing $p_l = 1 - p_r$ into the term proportional to $t$, and then making use of the linearity attribute of the anticipated value to simplify the formula, one obtains the results that are directly proportional to $t^2$.

$$\begin{aligned}
\mu(n_r^2) &= \left((2\mu(n_r)e)^2 - 2\left(2p_r\right) + t\right) + 4tp_r p_l \\
&= \left(2\mu(n_r^2) - t\right)^2 + 4tp_r p_l \\
&= \mu(2n_r - t)^2 + 4tp_r p_l \\
&= \mathbb{E}[X]^2 + 4tp_r p_l
\end{aligned} \tag{2.17}$$

The transition between the third and fourth lines occurs when the value of $x$ is equal to $n_r - n_l$, which may be expressed as $2n_r - t$. Given that $\sigma^2$ is equal to the average

of $x^2$ minus the square of the average of $x$, the square of the average of $x$ is removed from both sides of Equation (2.17) to obtain

$$\sigma^2 = 4tp_r p_l \tag{2.18}$$

The variance of the distribution is an important metric since it gives insight on;

$$\sigma \sim \sqrt{t} \tag{2.19}$$

This implies that, in a classical RW, the walker is expected to be at a distance of $O(\sqrt{t})$ from the origin. By the law of large numbers and the Central Limit Theorem, as $t$ increases the distribution of the simple RW at time $t$ converges to normal distribution with mean $0$ and standard deviation $\sqrt{t}$, $N(0, \sqrt{t})$ by using Equations (2.10), (2.19).

# CHAPTER 3

# QUANTUM WALK

## 3.1 Quantum Walk

Quantization is the typical method used to develop quantum models and formulate their equations. The operators that act on a HS reflect both momentum and energy, the dimension of which is determined by the number of degrees of freedom. A vector defined in a HS denotes the quantum system's state, and a unitary operation determines how it evolves, as long as the system remains completely unaffected by interactions. When the system is composed of many components, the tensor product of the HSs of each individual component is used to generate a HS. Systems built under quantum mechanics, which are not completely isolated from their surroundings may exhibit elements of randomness. Furthermore, a measurement on the quantum system at a certain moment is performed to gather information regarding it. This technique produces a distribution.

The tensor product of HSs is a pivotal concept in functional analysis and quantum mechanics, particularly in the study of composite quantum systems. Given two HSs $H_1$ and $H_2$, their tensor product, denoted as $H_1 \otimes H_2$, forms a new HS that encapsulates the combined structure of the two spaces. This construction is essential for describing systems where each subsystem is associated with a distinct HS, and the total system is represented by their tensor product.

İf $\{|e_i\rangle\}$ and $\{|f_j\rangle\}$ are orthonormal bases of the HSs $H_1$ and $H_2$, respectively, then the set $\{|e_i\rangle \otimes |f_j\rangle\}$ constitutes an orthonormal basis for the tensor product space $H_1 \otimes H_2$. Any vector $|\psi\rangle$ in $H_1 \otimes H_2$ can thus be expressed as a linear combination

of these basis elements:

$$|\psi\rangle = \sum_{i,j} c_{ij}|e_i\rangle \otimes |f_j\rangle, \tag{3.1}$$

where $c_{ij}$ are complex coefficients that describe the contribution of each basis element to the overall vector $|\psi\rangle$.

The inner product on $H_1 \otimes H_2$ is defined in a manner consistent with the inner products on the constituent spaces. Specifically, for vectors $|\psi\rangle = \sum_{i,j} c_{ij}|e_i\rangle \otimes |f_j\rangle$ and $|\phi\rangle = \sum_{k,l} d_{kl}|e_k\rangle \otimes |f_l\rangle$ in $H_1 \otimes H_2$, the inner product is given by:

$$\langle\psi|\phi\rangle = \sum_{i,j,k,l} c_{ij}^* d_{kl}\langle e_i|e_k\rangle\langle f_j|f_l\rangle, \tag{3.2}$$

where $c_{ij}^*$ denotes the complex conjugate of $c_{ij}$. This inner product structure ensures that $H_1 \otimes H_2$ inherits the properties of a HS, such as completeness and the ability to define orthonormal bases.

In quantum mechanics, the tensor product is particularly significant for describing composite systems. If two quantum systems are represented by the HSs $H_1$ and $H_2$, respectively, the total system is described by the tensor product space $H_1 \otimes H_2$. States in this combined space that can be written as simple tensor products $|\psi_1\rangle \otimes |\psi_2\rangle$, where $|\psi_1\rangle \in H_1$ and $|\psi_2\rangle \in H_2$, are called separable states. Conversely, states that cannot be decomposed into such a form are referred to as entangled states, which play a crucial role in quantum information theory.

Furthermore, operators on the tensor product space $H_1 \otimes H_2$ can often be expressed as tensor products of operators on $H_1$ and $H_2$. If $A$ is an operator on $H_1$ and $B$ is an operator on $H_2$, the operator $A \otimes B$ acts on the product space $H_1 \otimes H_2$ and is defined by its action on basis elements as $(A \otimes B)(|e_i\rangle \otimes |f_j\rangle) = (A|e_i\rangle) \otimes (B|f_j\rangle)$.

In quantum computing, a qubit is the basic unit of quantum information, represented by a vector in a two-dimensional HS, typically denoted as $\mathbb{C}^2$. The standard basis for this space is $\{|0\rangle, |1\rangle\}$, where:

$$|0\rangle = \begin{pmatrix} 1 \\ 0 \end{pmatrix}, \quad |1\rangle = \begin{pmatrix} 0 \\ 1 \end{pmatrix}. \tag{3.3}$$

Now, consider two qubits, with the first qubit in a state $|\psi_1\rangle$ and the second qubit in a

state $|\psi_2\rangle$. Suppose:

$$|\psi_1\rangle = \alpha|0\rangle + \beta|1\rangle, \quad |\psi_2\rangle = \gamma|0\rangle + \delta|1\rangle, \tag{3.4}$$

where $\alpha, \beta, \gamma, \delta$ are complex coefficients such that $|\alpha|^2+|\beta|^2 = 1$ and $|\gamma|^2+|\delta|^2 = 1$, ensuring that $|\psi_1\rangle$ and $|\psi_2\rangle$ are normalized.

The combined state of the two qubits is represented by the tensor product of their individual states:

$$|\psi_1\rangle \otimes |\psi_2\rangle = (\alpha|0\rangle + \beta|1\rangle) \otimes (\gamma|0\rangle + \delta|1\rangle). \tag{3.5}$$

Applying the distributive property of the tensor product, this expands to:

$$|\psi_1\rangle \otimes |\psi_2\rangle = \alpha\gamma|0\rangle \otimes |0\rangle + \alpha\delta|0\rangle \otimes |1\rangle + \beta\gamma|1\rangle \otimes |0\rangle + \beta\delta|1\rangle \otimes |1\rangle. \tag{3.6}$$

In the standard computational basis for the two-qubit system, $|0\rangle \otimes |0\rangle$, $|0\rangle \otimes |1\rangle$, $|1\rangle \otimes |0\rangle$, and $|1\rangle \otimes |1\rangle$ are typically written as $|00\rangle$, $|01\rangle$, $|10\rangle$, and $|11\rangle$, respectively. Therefore, the combined state can be expressed as:

$$|\psi_1\rangle \otimes |\psi_2\rangle = \alpha\gamma|00\rangle + \alpha\delta|01\rangle + \beta\gamma|10\rangle + \beta\delta|11\rangle. \tag{3.7}$$

Suppose:

$$|\psi_1\rangle = \frac{1}{\sqrt{2}}|0\rangle + \frac{1}{\sqrt{2}}|1\rangle, \quad |\psi_2\rangle = |0\rangle. \tag{3.8}$$

Here, $|\psi_1\rangle$ is an equal superposition of $|0\rangle$ and $|1\rangle$, and $|\psi_2\rangle = |0\rangle$.

The tensor product state is:

$$|\psi_1\rangle \otimes |\psi_2\rangle = \left(\frac{1}{\sqrt{2}}|0\rangle + \frac{1}{\sqrt{2}}|1\rangle\right) \otimes |0\rangle = \frac{1}{\sqrt{2}}|0\rangle \otimes |0\rangle + \frac{1}{\sqrt{2}}|1\rangle \otimes |0\rangle. \tag{3.9}$$

This simplifies to:

$$|\psi_1\rangle \otimes |\psi_2\rangle = \frac{1}{\sqrt{2}}|00\rangle + \frac{1}{\sqrt{2}}|10\rangle. \tag{3.10}$$

This state is now a vector in the four-dimensional HS $\mathbb{C}^2 \otimes \mathbb{C}^2$ corresponding to the two-qubit system. The coefficients $\frac{1}{\sqrt{2}}$ indicate that there is an equal probability of measuring the system in either the $|00\rangle$ or $|10\rangle$ state, and zero probability for the states $|01\rangle$ and $|11\rangle$.

The walker's position, denoted by $n$, represented as a HS vector $\mathcal{H}_P$ that has an infinite number of dimensions. HS's computational basis is given by the set $\{|n\rangle : n \in \mathbb{Z}\}$. Iteration of the process depends on the "quantum coin." If the result of flipping the "quantum coin" is "heads" and the current position is represented by the vector $|n\rangle$, in the next iteration, $|n+1\rangle$ will be next position. If the outcome is "tails," it will be represented by the state $|n-1\rangle$. Consider a particle as a "random walker". The particle's state is determined by both its position in the one-dimensional lattice and its spin, which can be either up or down. Therefore, the spin value has the ability to discern the direction of motion. If the particle is in the state represented by the position $|n\rangle$ and its spin is in the up direction, it will transition to the state represented by $|n+1\rangle$ while maintaining the same spin orientation. When the spin is in the down state, it should transition to the state $|n-1\rangle$. System's HS can be defined as the tensor product of two HSs, denoted as $\mathcal{H}_C$ and $\mathcal{H}_P$. Specifically, $\mathcal{H} = \mathcal{H}_C \otimes \mathcal{H}_P$. The HS $\mathcal{H}_C$ is a two-dimensional space that represents the "coin," and its computational basis is given by the states $|0\rangle$ and $|1\rangle$. The term "quantum coin" can be defined as a 2-dimensional unitary matrix, denoted as $C$, that operates on vectors in the HS $\mathcal{H}_C$. The term used to refer to "coin operator."

The shift operator describes transitions between different quantum states. In this context, a system where transitions occur between the states $|n\rangle$, $|n+1\rangle$, and $|n-1\rangle$ is considered. How the shift operator $S$ operates on the states $|n\rangle$ can be formally defined in terms of its effects:

$$\begin{aligned} S|0\rangle|n\rangle &= |0\rangle|n+1\rangle, \\ S|1\rangle|n\rangle &= |1\rangle|n-1\rangle. \end{aligned} \tag{3.11}$$

Equation (3.11) provides a detailed description of the shift operator $S$ by specifying its action on the computational basis states of the HS $\mathcal{H}$. It demonstrates that $S$ can be decomposed into two components: one that shifts states forward (associated with the $|0\rangle$ term) and one that shifts states backward (associated with the $|1\rangle$ term). This comprehensive characterization enables us to understand how $S$ operates on any state within the HS. Thus,

$$S = |0\rangle\langle 0| \otimes \sum_{n=-\infty}^{\infty} |n+1\rangle\langle n| + |1\rangle\langle 1| \otimes \sum_{n=-\infty}^{\infty} |n-1\rangle\langle n| \tag{3.12}$$

By applying $S$ to the states, the Equation (3.11) can be recovered. In QWs, the

process begins by applying $C$ on selected initial state, much as how a coin is tossed in classical walks. Each phrase inside this superposition will induce a shift in a distinct path. To achieve a symmetrical distribution over the starting location, a fair coin should be used. For this purpose, the selected coin state is $|0\rangle$, and the walk starts at position $|n = 0\rangle$.

$$|\psi(0)\rangle = |0\rangle|n = 0\rangle, \tag{3.13}$$

The symbol $|\psi(0)\rangle$ represents the initial state, while $|\psi(t)\rangle$ represents the state of the position quantum walker at time $t$.

The Hadamard operator is commonly used as the coin in the majority of one-dimensional QWs.

$$H = \frac{1}{\sqrt{2}} \begin{bmatrix} 1 & 1 \\ 1 & -1 \end{bmatrix} \tag{3.14}$$

A single step involves applying the $H$ operator to the state of the coin, specifically applying $H \otimes I$, where $I$ identity operator of HS $\mathcal{H}_P$, and then applying $S$.

$$|0\rangle \otimes |0\rangle \xrightarrow{H\otimes I} \frac{|0\rangle + |1\rangle}{\sqrt{2}} \otimes |0\rangle \xrightarrow{S} \frac{1}{\sqrt{2}}(|0\rangle \otimes |1\rangle + |1\rangle \otimes |-1\rangle). \tag{3.15}$$

The particle can be in either $n = 1$ or $n = -1$ since the particle in a superposition. This superposition arises from Hadamard Operator (Coin Operator). The Hadamard operator $H$ produces an unbiased result when acting on $|1\rangle$ and $|0\rangle$, as it produces equal amplitudes for both right and left positions. However, when $H$ is applied to $|1\rangle$, the amplitudes for right and left positions have different signs. Despite this, the sign difference does not affect the probability of finding the particle at a specific position, so $H$ can be referred as a non-biased coin.

To determine the particle's position, the state given by (3.15) is measured. Measuring in the computational basis of $\mathcal{H}_P$ will yield a $1/2$ probability of finding the particle at $n = 1$ and a $1/2$ probability at $n = -1$. This outcome mirrors the result of the first step in a classical RW. If $H$ and shift operator, and measure are repeatedly applied at each step, behavior characteristic of a classical RW will be observed. The main objective is to leverage quantum properties to achieve outcomes that are not possible in the classical physics. Quantum correlations between distinct locations, which are

common in quantum systems, are disrupted when the particle's position is measured after the initial step. By not measuring and instead applying the coin and shift operators successively, the quantum correlations are preserved, leading to constructive interference and resulting in behavior distinct from classical walks. Consequently, the standard deviation will not be $\sqrt{t}$ and will not converge to normal distribution.

The QW involves iteratively applying the unitary operator several times without doing measurements. $U$ defined as,

$$U = S(H \otimes I). \tag{3.16}$$

Then, the position state of quantum walker will be after one step iteration,

$$|\psi(t+1)\rangle = U|\psi(t)\rangle. \tag{3.17}$$

In our case, the walk start at position $n = 0$ with coin state $|0\rangle$ given in (3.13). The position state of the QW after one step iteration becomes,

$$|\psi(1)\rangle = U|\psi(0)\rangle. \tag{3.18}$$

After $t$ step, the position state is described by

$$|\psi(t)\rangle = U^t|\psi(0)\rangle. \tag{3.19}$$

Let us start by accurately calculating the initial stages in order to have a comprehensive comparison with the traditional RW. To calculate the first step, use the formula $|\psi(1)\rangle = U|\psi(0)\rangle$ and continue this procedure for following stages.

$$\begin{aligned}
|\psi(1)\rangle &= \frac{1}{\sqrt{2}}(|1\rangle|-1\rangle + |0\rangle|1\rangle) \\
|\psi(2)\rangle &= \frac{1}{2}(-|1\rangle|-2\rangle + (|0\rangle + |1\rangle)|0\rangle + |0\rangle|2\rangle) \\
|\psi(3)\rangle &= \frac{1}{2\sqrt{2}}(|1\rangle|-3\rangle - |0\rangle|-1\rangle + (2|0\rangle + |1\rangle)|1\rangle + |0\rangle|3\rangle)
\end{aligned} \tag{3.20}$$

By following these preliminary calculations, it can be seen that, the QW and simple RW differ in many ways throughout the path. For example, although an unbiased coin is used in our experiment, the quantum state $|\psi(3)\rangle$ does not display symmetry around the origin. In Figure 3.1, the distribution of the process was shown without

| $t$ \ $n$ | $-5$ | $-4$ | $-3$ | $-2$ | $-1$ | $0$ | $1$ | $2$ | $3$ | $4$ | $5$ |
|---|---|---|---|---|---|---|---|---|---|---|---|
| 0 | | | | | | 1 | | | | | |
| 1 | | | | | $\frac{1}{2}$ | | $\frac{1}{2}$ | | | | |
| 2 | | | | $\frac{1}{4}$ | | $\frac{1}{2}$ | | $\frac{1}{4}$ | | | |
| 3 | | | $\frac{1}{8}$ | | $\frac{1}{8}$ | | $\frac{5}{8}$ | | $\frac{1}{8}$ | | |
| 4 | | $\frac{1}{16}$ | | $\frac{1}{8}$ | | $\frac{1}{8}$ | | $\frac{5}{8}$ | | $\frac{1}{16}$ | |
| 5 | $\frac{1}{32}$ | | $\frac{5}{32}$ | | $\frac{1}{8}$ | | $\frac{1}{8}$ | | $\frac{17}{32}$ | | $\frac{1}{32}$ |

Figure 3.1: Chance of finding the walker at position $n$ at time $t$, starting from origin with coin in "heads" state and without any intermediate measurements, can be determined. This involves applying the operator $U$ once. The operator $U$ is repeatedly applied without making any measurements in between. At a specific time $t$, the state describes the distribution of position of particle.

any intermediate measurements. Besides its asymmetry property, the location of the distribution is not at the origin. This can be clearly illustrated by comparing it with the table given in Figure 3.1.

Our aim is to determine the distribution of a process with large number of steps. However, the current method used is not suitable for manual calculations. For instance, to find $p(100, n)$, which represents the distribution at the hundredth step, compute the absolute value of the wave function at position 100, $|\psi(100)\rangle$ needs to be computed. Yusuf Karli [14], has shown analytical solution for QW in this purpose. In order to generalize, $\sigma$ symbol will be used to represent the coin state. If the shift operator $S$ is adjusted with respect to $\sigma$, we have,

$$S = \sum_{\sigma=0}^{1} \sum_{n=-\infty}^{\infty} |\sigma, n + (-1)^{\sigma}\rangle \langle \sigma, n| \tag{3.21}$$

A QW is considered a non-Markovian process because its evolution is inherently dependent on the initial state of the quantum coin, which differentiates it from classical RWs. In classical Markovian processes, the future state depends only on the present state and not on the sequence of events that preceded it. However, in a QW, the superposition and entanglement of the quantum states introduce memory effects where the entire history of the system's evolution, particularly the initial coin state, influences the probabilities of future outcomes. This memory dependency makes QWs

non-Markovian, allowing for more complex and rich dynamics compared to their classical counterparts. The position state of the walk at $t^{th}$-step can be described with probability amplitudes. Thus, the position state can be represented as,

$$\left|\psi^{\sigma'}(t)\right\rangle = \sum_{n,\sigma} A^{\sigma'}_{n\sigma}(t)|n\rangle|\sigma\rangle, \tag{3.22}$$

Where, the probability amplitude coefficients satisfy the normalization condition.

$$\sum_{z} \left|A^{\sigma'}_{x0}(t)\right|^2 + \left|A^{\sigma'_1}_{x1}(t)\right|^2 = 1 \tag{3.23}$$

Now, the distribution for walker at position $n$ and time $t$ can be calculated using the formula,

$$\Pr(n,t) = \sum_{\sigma} \left|A^{\sigma'}_{x\sigma}(t)\right|^2. \tag{3.24}$$

To find the analytical solution for the distribution of the walk, given the initial coin state $\sigma = 0$, we refer to Equation (3.13). It can be shown as,

$$|\psi(t+1)\rangle = \sum_{n} S\left(A_{z,0}(t)C|0,n\rangle + A_{z,1}(t)C|1,n\rangle\right). \tag{3.25}$$

Where $C$ represents the coin operator, which is used to manipulate the coin states in the QW. Specifically, in this case, the coin operator $C$ is the Hadamard operator. The Hadamard operator $H$ is a quantum operation that acts on the coin states, which are typically represented as $|0\rangle$ and $|1\rangle$.

When the Hadamard operator is applied, it maps the coin states into a superposition state. This means that the state of the coin is no longer just $|0\rangle$ or $|1\rangle$; instead, it becomes a combination of both states with equal probability amplitudes. This can be expressed as follows:

$$H|0\rangle = \frac{1}{\sqrt{2}}(|0\rangle + |1\rangle) \tag{3.26}$$

$$H|1\rangle = \frac{1}{\sqrt{2}}(|0\rangle - |1\rangle) \tag{3.27}$$

This operation creates a balanced superposition, where the coin has an equal probability of being in either state $|0\rangle$ or $|1\rangle$. This superposition is a key aspect of QWs, as

it introduces quantum interference effects that influence the walk's distribution.

$$\sum_n \frac{1}{\sqrt{2}} \left(A_{n,0}(t) + A_{n,1}(t)\right) S|0,n\rangle + \frac{1}{\sqrt{2}} \left(A_{n,0}(t) - A_{n,1}(t)\right) S|1,n\rangle \tag{3.28}$$

By using definition given in Equation (3.21), the shift operator $S$ determines the walker's movement based on the selected coin state.

$$\sum_n \frac{1}{\sqrt{2}} \left(A_{n,0}(t) + A_{n,1}(t)\right) |0,n+1\rangle + \frac{1}{\sqrt{2}} \left(A_{n,0}(t) - A_{n,1}(t)\right) |1,n-1\rangle \tag{3.29}$$

By regrouping terms with the same indices, the probability amplitudes are expressed for $\mathrm{n}+1$. Then,

$$\begin{aligned} A_{n,0}(t+1) &= \frac{1}{\sqrt{2}} \left(A_{n-1,0}(t) + A_{n-1,1}(t)\right) \\ A_{n,0}(t+1) &= \frac{1}{\sqrt{2}} \left(A_{n+1,0}(t) - A_{n+1,1}(t)\right) \end{aligned} \tag{3.30}$$

using Fourier transform,

$$\tilde{A}_{k,\sigma}(t) = \sum_{n=-\infty}^{\infty} e^{-ikn} A_{n,\sigma}(t) \tag{3.31}$$

Then $|k\rangle$ can be defined in terms of $|n\rangle$,

$$|k\rangle = \sum_n e^{ikn} |n\rangle. \tag{3.32}$$

Thus, at time $t$, the position state of the walk can be rewritten as,

$$|\psi(t)\rangle = \int_{-\pi}^{\pi} \frac{dk}{2\pi} \sum_\sigma \tilde{A}_{k,\sigma} |\sigma,k\rangle. \tag{3.33}$$

After arranging the position state, unitary operator $U$ can be applied starting with by applying $S$ operator to the $|\sigma,k\rangle$.

$$\begin{aligned} S|\sigma,k\rangle &= \sum_n e^{ikn} S|\sigma,n\rangle \\ S|\sigma,k\rangle &= \sum_n e^{ikn} |\sigma,n+(-1)^\sigma\rangle \end{aligned} \tag{3.34}$$

By modifying the indices $n' = n + (-1)^\sigma$, $n = n' - (-1)^\sigma$. Thus,,

$$S|\sigma,k\rangle = \sum_{n'} e^{ik(x'-(-1)^\sigma)} S\,|\sigma,n'\rangle\,. \tag{3.35}$$

The vector $|k\rangle$ can be written as $e^{ikn'}\,|n'\rangle$.Thus,

$$S|\sigma,k\rangle = \sum_{n'} e^{ik(-(-1)^{\sigma})} S|\sigma,k\rangle \tag{3.36}$$

It is seen that the phase of the position state is altered by the shift operator. The evolution operator can be defined for each $k$ with following equation:

$$\tilde{U}_k = \begin{pmatrix} e^{-ik} & 0 \\ 0 & e^{ik} \end{pmatrix} C. \tag{3.37}$$

$C$ is representing Hadamard coin. To diagonalize the matrix $\tilde{U}_k$, start by deriving its characteristic polynomial. The matrix $\tilde{U}_k$ is defined as follows:

$$\tilde{U}_k = \frac{1}{\sqrt{2}} \begin{pmatrix} e^{-ik} & e^{-ik} \\ e^{ik} & -e^{ik} \end{pmatrix} \tag{3.38}$$

The first step in diagonalization involves finding the eigenvalues of $\tilde{U}_k$. This requires calculating the characteristic polynomial, which is obtained by subtracting $\lambda$, a scalar corresponding to an eigenvalue, from the diagonal elements of $\tilde{U}_k$ and subsequently determining the determinant of the resulting matrix. Thus, the matrix $\tilde{U}_k - \lambda I$, where $I$ denotes the identity matrix, is given by,

$$\tilde{U}_k - \lambda I = \begin{pmatrix} \frac{e^{-ik}}{\sqrt{2}} - \lambda & \frac{e^{-ik}}{\sqrt{2}} \\ \frac{e^{ik}}{\sqrt{2}} & -\frac{e^{ik}}{\sqrt{2}} - \lambda \end{pmatrix} \tag{3.39}$$

The next step involves calculating the determinant of the matrix $\tilde{U}_k - \lambda I$ to formulate the characteristic polynomial. The determinant of a $2 \times 2$ matrix, $\begin{pmatrix} a & b \\ c & d \end{pmatrix}$, is computed as $ad - bc$. Applying this to our matrix:

$$\det(\tilde{U}_k - \lambda I) = \left(\frac{e^{-ik}}{\sqrt{2}} - \lambda\right)\left(-\frac{e^{ik}}{\sqrt{2}} - \lambda\right) - \frac{e^{-ik}}{\sqrt{2}} \cdot \frac{e^{ik}}{\sqrt{2}} \tag{3.40}$$

Expanding the first product,

$$\left(\frac{e^{-ik}}{\sqrt{2}} - \lambda\right)\left(-\frac{e^{ik}}{\sqrt{2}} - \lambda\right) = -\frac{1}{2} - \lambda\frac{e^{-ik}}{\sqrt{2}} + \lambda\frac{e^{ik}}{\sqrt{2}} + \lambda^2 \tag{3.41}$$

is ontained. The determinant thus simplifies to:

$$\det(\tilde{U}_k - \lambda I) = -\frac{1}{2} - \lambda\frac{e^{-ik}}{\sqrt{2}} + \lambda\frac{e^{ik}}{\sqrt{2}} + \lambda^2 - \frac{1}{2} \tag{3.42}$$

Then, combining the constant terms yields the characteristic polynomial:

$$\det(\tilde{U}_k - \lambda I) = -1 + \lambda^2 - \lambda\frac{e^{-ik}}{\sqrt{2}} + \lambda\frac{e^{ik}}{\sqrt{2}} \tag{3.43}$$

The roots of the characteristic polynomial, corresponding to the eigenvalues $\lambda$, are essential for the diagonalization of $\tilde{U}_k$. Once the eigenvalues are determined, they can be used to transform $\tilde{U}_k$ into its diagonal form, thereby elucidating its spectral properties. To diagonalize the matrix $\tilde{U}_k$, start by expressing the characteristic polynomial using the exponential form of the sine function. Given:

$$\sin k = \frac{e^{ik} - e^{-ik}}{2i}, \tag{3.44}$$

the characteristic polynomial simplifies to:

$$\lambda^2 + \sqrt{2}\lambda i \sin k - 1. \tag{3.45}$$

By substituting the exponential form of $\sin k$ into the polynomial,

$$\lambda^2 + \sqrt{2}\lambda i\frac{e^{ik} - e^{-ik}}{2i} - 1. \tag{3.46}$$

is obtained.

Simplifying, this results in the characteristic polynomial:

$$\lambda^2 + \sqrt{2}\lambda\frac{e^{ik} - e^{-ik}}{2} - 1. \tag{3.47}$$

In order to find the eigenvalues, this quadratic equation is solved and the eigenvalues are:

$$a_1 = e^{-i\omega_k}, \quad a_2 = e^{i(\pi+\omega_k)}, \tag{3.48}$$

where $\omega_k$ is a phase angle derived from the parameters of the problem. Next, the eigenvectors associated with these eigenvalues are determined.

For the eigenvalue $a_1 = e^{-i\omega_k}$, the corresponding eigenvector is:

$$|a_1\rangle = \frac{1}{\sqrt{c^-}} \begin{pmatrix} e^{-ik} \\ \sqrt{2}e^{-i\omega_k} - e^{-ik} \end{pmatrix}, \tag{3.49}$$

where $c^-$ is a normalization constant ensuring that $|a_1\rangle$ is properly normalized.

Similarly, for the eigenvalue $a_2 = e^{i(\pi+\omega_k)}$, the eigenvector is:

$$|a_2\rangle = \frac{1}{\sqrt{c^+}} \begin{pmatrix} e^{-ik} \\ -\sqrt{2}e^{i\omega_k} - e^{-ik} \end{pmatrix}, \tag{3.50}$$

where $c^+$ is another normalization constant.

Using definitions,

$$\omega_k = \arcsin\left(\frac{1}{\sqrt{2}}\sin k\right), \tag{3.51}$$

$$\frac{1}{c^\pm} = \frac{1}{2}\left(1 \mp \frac{\cos k}{\sqrt{1+\cos^2 k}}\right), \tag{3.52}$$

The unitary operator can be rewritten as,

$$U^t = \int_{-\pi}^{\pi} \frac{dk}{2\pi} e^{-i\omega_k t} |a_1\rangle |k\rangle \langle k| \left\langle a_1 \right| + e^{i(\pi+\omega_k)t} \left| a_2 \right\rangle |k\rangle \langle k| \langle a_2| \tag{3.53}$$

Where $|k\rangle$ is,

$$|k\rangle = \sum_{n=-\infty}^{\infty} e^{ikn} |n\rangle. \tag{3.54}$$

The position state after $t$ step iteration will be,

$$|\psi(t)\rangle = U^t |\psi(0)\rangle. \tag{3.55}$$

Since our initial state is $|\psi(0)\rangle = |\sigma = 0\rangle|x = 0\rangle$, the position state at $t^{th}$-step is,

$$|\psi_t\rangle = \left[\int_{-\pi}^{\pi} \frac{dk}{2\pi} e^{-i\omega_k t} |a_1\rangle |k\rangle \langle k| \left\langle a_1 \right| + e^{i(\pi+\omega_k)t} \left| a_2 \right\rangle |k\rangle \langle k| \langle a_2|] \mid \sigma = 0\rangle |x = 0\rangle \tag{3.56}$$

Using the eigenvectors given in (3.48) and (3.49), the position state $|\psi(t)\rangle$ will be,

$$|\psi_t\rangle = \left[\int_{-\pi}^{\pi} e^{-i\omega_k t} \frac{e^{ik}}{\sqrt{c^-}} |a_1\rangle + e^{i(\pi+\omega_k)t} \frac{e^{ik}}{\sqrt{c^+}} |a_2\rangle\right] |k\rangle \frac{dk}{2\pi} \tag{3.57}$$

$$|\psi(t)\rangle = \left[\int_{-\pi}^{\pi} e^{-i\omega_k t+ik}\frac{1}{c^-}\begin{pmatrix} e^{-ik} \\ \sqrt{2}e^{-i\omega_k} - e^{-ik}\end{pmatrix} + e^{i(\pi+\omega_k)t+ik}\frac{1}{c^+}\begin{pmatrix} e^{-ik} \\ -\sqrt{2}e^{i\omega_k} - e^{-ik}\end{pmatrix}\right]|k\rangle\frac{dk}{2\pi} \tag{3.58}$$

Finally, the probability amplitudes for the selected initial coin state $\sigma = 0$ are,

$$A^0_{k0}(t) = \frac{1}{c^-}e^{-i\omega_k t} + \frac{1}{c^+}e^{i(\pi+\omega_k)t} \tag{3.59}$$

$$A^0_{k1}(t) = \frac{1}{c^-}e^{-i\omega_k t+ik}\left(\sqrt{2}e^{-i\omega_k} - e^{-ik}\right) - \frac{1}{c^+}e^{i(x+\omega_k)t+ik}\left(\sqrt{2}e^{i\omega_k} + e^{-ik}\right) \tag{3.60}$$

The probability amplitudes in real space can be found by taking inverse Fourier transform as follows:

$$A^{\sigma'}_{n\sigma}(t) = \int_{-\pi}^{\pi}\frac{dk}{2\pi}e^{ikn}A^{\sigma'}_{k\sigma}(t) \tag{3.61}$$

A different strategy involves directly calculating matrix $U$, [21]. The tensor product is essential for constructing shift operator, as described in Equation (3.21). These operators manipulate vectors in an infinite vector space. However, the number of non-zero elements is restricted. Therefore, it is imperative for these arrays to possess dimensions that exceed slightly the size of $200 \times 200$. After calculating the value of $U$, $U^{100}$ can be calculated and multiply it by the initial condition $|\psi(0)\rangle$, which is represented as a column vector with an appropriate number of components. The result is the state vector $|\psi(100)\rangle$. Finally, we are able to calculate the distribution.

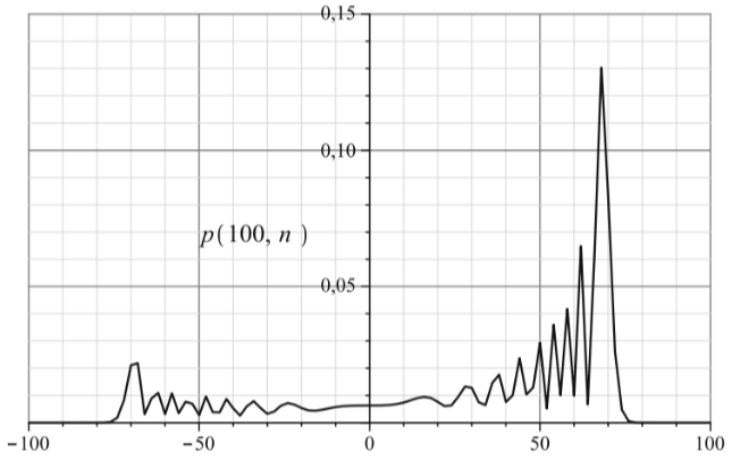



Figure 3.2: Frequency plot for initial condition $|\psi(0)\rangle = |1\rangle|n = 0\rangle$. [21]

Using previously mentioned methods, one can acquire plot shown in Figure (**??**). Like the simple RW, the probability values that are equal to zero should be ignored. At time $t = 100$, the probability is zero for every odd value of $n$. The presence of asymmetry in the distribution is clearly apparent. The chance of locating the particle to right of the origin is greater than the chance of locating it to left. More precisely, when the value of $n$ is about equal to $100/\sqrt{2}$, the probability is considerably higher compared to when it is at the starting point. It is not restricted to the particular value of $t = 100$ as the method is suitable for every $t$. This shows the QW has a ballistic behavior. Walker can be situated at a distance from the origin, appearing to move uniformly in rightward direction. Therefore, one can question whether this pattern would remain consistent if the distribution was symmetrically centered around the origin.

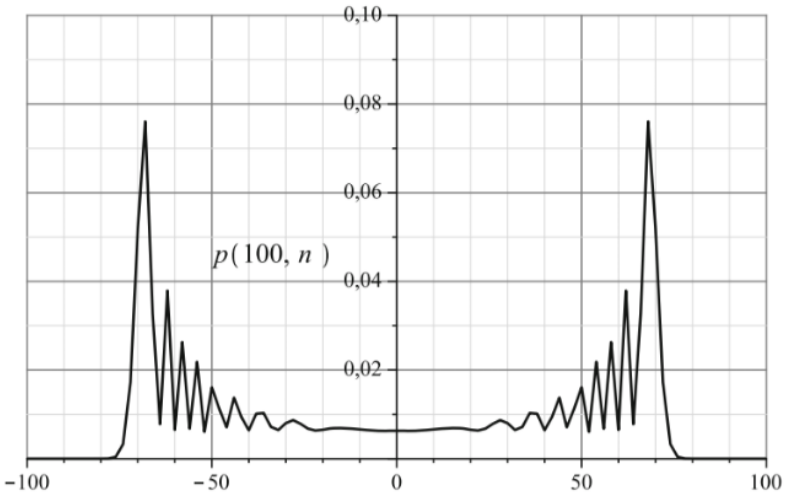



Figure 3.3: Frequency plot after 100 steps for symmetric QW. [21]

In order to attain a symmetrical distribution, it is imperative to understand the underlying cause for the observed rightward tendency in the prior instance. Applying the Hadamard coin to state $|1\rangle$ results in the introduction of a negative sign. This suggests that there is a higher frequency of cancellations for states that have a coin state of $|1\rangle$ compared to terms with a coin state of $|0\rangle$. As the coin state $|0\rangle$ causes movement to right and $|1\rangle$ causes movement to left, the result is an asymmetry with a considerably larger probability on right side. In order to verify the effectiveness of this method, we

can calculate the resulting distribution based on the original condition.

$$|\psi(0)\rangle = -|1\rangle|n=0\rangle. \tag{3.62}$$

In this scenario, the quantity of negative terms will exceed that of positive terms, resulting in a greater number of term cancellations involving the coin state $|0\rangle$. The ultimate outcome will be the symmetrical distribution depicted in figure (3.3) with respect to the vertical axis. In order to achieve a symmetrical distribution, it is necessary to overlay the QWs that arise from these two beginning conditions. The superposition should not eliminate terms prior to calculating the distribution. To obtain the desired result, one needs to multiply the complex $i$ by the second initial condition and then add it to the first initial condition, as shown below:

$$|\psi(0)\rangle = \frac{|0\rangle - i|1\rangle}{\sqrt{2}}|n=0\rangle. \tag{3.63}$$

Hadamard operator consist of real numbers. Using the evolution operator does not convert terms involving the imaginary unit into real terms, nor does it convert real terms into terms involving the imaginary unit. There will be no simplification of terms between rightward walk and leftward walk. Finally, the distributions are combined. The outcome is the visual representation depicted in Figure (3.3)

Note that, whenever QW distribution shows symmetry, the position's expectation will be zero, denoted as $\mu(n) = 0$.

Following R code perform simulation by calculating matrix $U$. However, MATLAB code for analytical solution can be found in [14].

```
QRW    function(steps,initialstate)
  line    steps 2  + 1
  I    diag(line)
  H    cbind(c(1/sqrt(2),1/sqrt(2)),c(1/sqrt(2) , 1/sqrt(2)))
  U    kronecker(H,I)
  S1    matrix(0,ncol = line,nrow = line)
  for (i in line:2)
    S1    as.matrix(I[,i 1])   t(as.matrix(I[,i])) + S1
  S1    as.matrix(I[,line])   t(as.matrix(I[,1])) + S1
  S1    kronecker(matrix(c(0,1),ncol=1)     matrix(c(0,1),nrow =1),S1)
  S2    matrix(0,ncol = line,nrow = line)
  for (i in 1:(line 1))
    S2    as.matrix(I[,i+1])   t(as.matrix(I[,i])) + S2
  S2    as.matrix(I[,1])   t(as.matrix(I[,line])) + S2
  S2    kronecker(matrix(c(1,0),ncol=1)     matrix(c(1,0),nrow =1),S2)
  S    S1 + S2
  Y    S   U
  initial    kronecker(matrix(initialstate,ncol=1),as.matrix(I[,steps+1]))
  state    Y   initial
  if (steps   1)
    for (i in 2:steps)
      state    Y   state


  prob    as.matrix(state[1:line,]2+state[(line+1):dim(state)[1],]2 )
  colnames(prob)    "prob"
  return(prob)

k    0
j    k
l    c(k)
for (i in 1:100)
  prob    QRW(i,c(1,0))
  while((j 1) != k   k != (j+1))
    k    sample( i:i,1,replace = TRUE,prob = as.vector(prob))

  l[i+1]    k
  j    k

plot(l)
lines(l)
l2    c()
for (t in 1:1000)
  k    0
  j    k
  l    c(k)
  for (i in 1:100)
    prob    QRW(i,c(1,0))
    while((j 1) != k   k != (j+1))
      k    sample( i:i,1,replace = TRUE,prob = as.vector(prob))

    l[i+1]    k
    j    k

  l2[t]    l[101]
  print(l[101])

hist(l2,breaks = 100)
```

# CHAPTER 4

# SIMULATION

## 4.1 Computations Regarding Quantum Walk

In this chapter, the study primarily builds upon concepts discussed in [26].

First, an unitary matrix is defined for $x \in \mathbb{Z}$,

$$C_x = \begin{bmatrix} a_x & b_x \\ c_x & d_x \end{bmatrix}, \tag{4.1}$$

where $a_x, b_x, c_x, d_x \in \mathbb{C}$ and $a_x b_x c_x d_x \neq 0$. It is called $C_x$ coin operator (Coin Matrix) for the QW. Decomposition of $C$ is done by using two vectors; $|\mathrm{L}\rangle = \begin{bmatrix} 1 & 0 \end{bmatrix}^\top$ and $|\mathrm{R}\rangle = \begin{bmatrix} 0 & 1 \end{bmatrix}^\top$. By using these,

$$P_x = |\mathrm{L}\rangle \langle \mathrm{L}\,| C_x, \quad Q_x = |\,\mathrm{R}\rangle \langle \mathrm{R}| C_x. \tag{4.2}$$

Then, the decomposition of $C_x$

$$C_x = P_x + Q_x. \tag{4.3}$$

$P_x$ and $Q_x$ representing left and right or transition probabilities in relation to classic RWs, respectively.

The vector $\Psi_n(x)$ is a probability amplitude vector, which means it contains information about the quantum walker's state at position $x$ at time $n$. $(n, x) \in \mathbb{N}_0 \times \mathbb{Z}$ indicates that $n$ is a non-negative integer corresponding to the time step of the QW,

and $x$ is an integer representing the position on a one-dimensional lattice. The components of $\Psi_n(x)$ are complex numbers that describe the likelihood (amplitude) of the walker being at position $x$ at time $n$, along with the phase information, which is crucial for understanding quantum interference effects, [26]. The walk over time is iterated by using equation,

$$\Psi_{n+1}(x) = P_{x+1}\Psi_n(x+1) + Q_{x-1}\Psi_n(x-1), \tag{4.4}$$

This is similar to the method used to calculate the probability of a walker's existence in classical RWs.

$$\mu_n(x) = \|\Psi_n(x)\|^2, \tag{4.5}$$

The symbol $\mu_n(x)$ denotes the probability of measuring the particle at point $x$ at time $n$.

The transition probabilities in a RW are defined by a specific quantity for each pair $(n, x)$ in $\mathbb{N}_0 \times \mathbb{Z}$, with the condition that $\mu_n(x)$ is greater than zero, [26].

$$p_n(x) = \frac{\|P_x\Psi_n(x)\|^2}{\mu_n(x)}, \quad q_n(x) = \frac{\|Q_x\Psi_n(x)\|^2}{\mu_n(x)}. \tag{4.6}$$

In [26], they gave definitions for $p_n(x)$ and $q_n(x)$ which is crucial for constructing the distributions.

Given a pair $(n, x)$ where $n$ is a non-negative integer ($\mathbb{N}_0$) and $x$ is an integer ($\mathbb{Z}$), the measure $\mu_n(x)$ is positive. Additionally, the probabilities $p_n(x)$ and $q_n(x)$ are both restricted within the interval $[0, 1]$.

$$0 \leq p_n(x) \leq 1 \quad \text{and} \quad 0 \leq q_n(x) \leq 1 \tag{4.7}$$

The non-negativity of $p_n(x)$, follows directly from the properties of norms and the assumption $\mu_n(x) > 0$, [26]. This ensures that

$$0 \leq p_n(x). \tag{4.8}$$

To demonstrate the upper bound, introduce the vector $\langle P_{\mathrm{L}}| = [a_x, b_x]$, leading to the relation $\|P\Psi_n(x)\|^2 = |\langle P_{\mathrm{L}} \mid \Psi_n(x)\rangle|^2$. By invoking the Cauchy-Schwarz inequality,

$$|\langle P_{\mathrm{L}} \mid \Psi_n(x)\rangle|^2 \leq \|P_{\mathrm{L}}\|^2 \cdot \|\Psi_n(x)\|^2 . \tag{4.9}$$

is obtained.

Since the coin operator $C$ is unitary, it follows that $\|P_{\mathrm{L}}\|^2 = 1$, leading to the inequality $\|P\Psi_n(x)\|^2 \leq \mu_n(x)$. Consequently, the probability $p_n(x)$, defined as the ratio $\frac{\|P\Psi_n(x)\|^2}{\mu_n(x)}$, is bounded above by 1, i.e., $p_n(x) \leq 1$. Thus, combining results for non-negativity and the upper bound, it is concluded that $p_n(x)$ lies within interval $[0, 1]$, [26].

A similar argument can be applied to $q_n(x)$, utilizing same reasoning based on norm properties, Cauchy-Schwarz inequality, and unitarity of coin operator. Hence, both $p_n(x)$ and $q_n(x)$ are probabilities, properly bounded between $0$ and $1$.

Lemma 2,[26]. A QW at a given time $n$ and position $x$ where $\mu_n(x) > 0$, the sum of probabilities $p_n(x)$ and $q_n(x)$ equals 1, i.e., $p_n(x) + q_n(x) = 1$.

Proof. Due to unitarity of coin operator $C$, the norm of quantum state is preserved under its action. Specifically, for a quantum walker's state $\Psi_n(x)$, the measure $\mu_n(x)$ is given by the squared norm $\|\Psi_n(x)\|^2$, which remains unchanged when coin operator is applied:

$$\mu_n(x) = \|\Psi_n(x)\|^2 = \|C_x\Psi_n(x)\|^2 = \|P_x\Psi_n(x) + Q_x\Psi_n(x)\|^2 . \tag{4.10}$$

The projection operators $P_x$ and $Q_x$ project onto orthogonal states $\mid \mathrm{L}\rangle$ and $\mid \mathrm{R}\rangle$, respectively. Given that $\langle \mathrm{L} \mid \mathrm{R}\rangle = \langle \mathrm{R} \mid \mathrm{L}\rangle = 0$, cross terms vanish, allowing us to simplify the norm as follows:

$$\|P_x\Psi_n(x) + Q_x\Psi_n(x)\|^2 = \|P_x\Psi_n(x)\|^2 + \|Q_x\Psi_n(x)\|^2 . \tag{4.11}$$

Therefore, the total norm $\mu_n(x)$ is the sum of squared norms associated with projec-

tions onto $|\,\mathrm{L}\rangle$ and $|\,\mathrm{R}\rangle$:

$$\|P_x\Psi_n(x)\|^2 + \|Q_x\Psi_n(x)\|^2 = \mu_n(x). \tag{4.12}$$

Dividing by $\mu_n(x)$ yields:

$$\frac{\|P_x\Psi_n(x)\|^2}{\mu_n(x)} + \frac{\|Q_x\Psi_n(x)\|^2}{\mu_n(x)} = 1, \tag{4.13}$$

which simplifies to $p_n(x) + q_n(x) = 1$.

Based on the above lemmas, The Quantum-Walk-Replicating Random Walk can be defined as follows:

The QW $\{\Psi_n\}_{n\in\mathbb{N}_0}$ is defined by a specific recurrence relation that governs its time evolution. At each time step $n$, the state of quantum walker at position $x$ is given by $\Psi_{n+1}(x)$, which is determined as a linear combination of the quantum walker's state from neighboring positions at previous time step,[26]. Specifically, the state $\Psi_{n+1}(x)$ is formed by the sum of projections of the state $\Psi_n(x+1)$ from position $x+1$ and $\Psi_n(x-1)$ from position $x-1$ under operators $P_{x+1}$ and $Q_{x-1}$, respectively.

$$\Psi_{n+1}(x) = P_{x+1}\Psi_n(x+1) + Q_{x-1}\Psi_n(x-1). \tag{4.14}$$

The initial condition is provided by $\Psi_0(x) = \delta_0(x)\varphi_0$, where $\delta_0(x)$ is Dirac delta function centered at $x = 0$ and $\varphi_0$ is a normalized initial state with $\|\varphi_0\| = 1$.

**The Quantum-Walk-Replicating Random Walk (QWRW):** $\{S_n\}_{n\in\mathbb{N}_0}$ is a classical RW that replicates the behavior of QW by using probabilities derived from the QW's state. The transition probabilities for QWRW are defined as follows: at each time step $n$ and position $x$, walker's probability moving to position $x+1$ or $x-1$ at next time step $n+1$ is given by $q_n(x)$ or $p_n(x)$, respectively. These probabilities are derived from squared norms of the projection of quantum state at position $x$ under operators $P_x$ and $Q_x$, normalized by the total probability amplitude $\mu_n(x)$:

$$\mathbb{P}(S_{n+1} = x + \xi \mid S_n = x) = \begin{cases} p_n(x) & \text{if } \xi = -1 \\ q_n(x) & \text{if } \xi = +1 \\ 0 & \text{otherwise.} \end{cases} \tag{4.15}$$

Here, $p_n(x) = \frac{\|P_x \Psi_n(x)\|^2}{\mu_n(x)}$ and $q_n(x) = \frac{\|Q_x \Psi_n(x)\|^2}{\mu_n(x)}$, ensuring that transition probabilities are consistent with the underlying QW.

The distribution $\nu_n(x)$ represents the likelihood of finding the QWRW particle at position $x$ at time $n$. This distribution evolves according to a recurrence relation similar to that of QW, where the probability at a given position $x$ at time $n+1$ is determined by probabilities of being at neighboring positions $x+1$ and $x-1$ at previous time step, weighted by corresponding transition probabilities $p_n(x)$ and $q_n(x)$:

$$\nu_{n+1}(x) = p_n(x+1)\nu_n(x+1) + q_n(x-1)\nu_n(x-1). \tag{4.16}$$

This equation captures how distribution shifts over time as the QWRW particle moves through different positions on the integer line, [26].

Finally, the distribution of QWRW across all possible positions at time $n$ is encapsulated in the vector $\nu_n$, which is defined as:

$$\nu_n = [\cdots, \nu_n(-1), \nu_n(0), \nu_n(1), \cdots]^\top. \tag{4.17}$$

This vector contains probabilities of the QWRW particle being at each integer position on the line $\mathbb{Z}$ at time $n$, providing a comprehensive view of the particle's distribution across space as RW progresses.

Lemma 4, [26]. For any non-negative integer $n$, the probability amplitude $\mu_{n+1}(x)$ at time $n+1$ and position $x$ can be expressed as a linear combination of the probability amplitudes from neighboring positions $x+1$ and $x-1$ at previous time step $n$, weighted by transition probabilities $p_n(x+1$ and $q_n(x-1)$, respectively.

$$\mu_{n+1}(x) = p_n(x+1)\mu_n(x+1) + q_n(x-1)\mu_n(x-1). \tag{4.18}$$

Proof. Recalling that $\mu_{n+1}(x)$, which represents the probability amplitude at position $x$ at time $n+1$, is the squared norm of the quantum state $\Psi_{n+1}(x)$:

$$\mu_{n+1}(x) = \|\Psi_{n+1}(x)\|^2. \tag{4.19}$$

According to QW's evolution equation, $\Psi_{n+1}(x)$ is the sum of projections of quantum states from neighboring positions $x+1$ and $x-1$ at time $n$, transformed by operators $P_{x+1}$ and $Q_{x-1}$, respectively:

$$\Psi_{n+1}(x) = P_{x+1}\Psi_n(x+1) + Q_{x-1}\Psi_n(x-1). \tag{4.20}$$

To find $\mu_{n+1}(x)$, take the squared norm of this sum:

$$\mu_{n+1}(x) = \|P_{x+1}\Psi_n(x+1) + Q_{x-1}\Psi_n(x-1)\|^2. \tag{4.21}$$

This squared norm can be expanded using linearity of inner products:

$$\begin{aligned}
\mu_{n+1}(x) = \|\Psi_{n+1}(x)\|^2 &= \|P_{x+1}\Psi_n(x+1) + Q_{x-1}\Psi_n(x-1)\|^2 \\
&= \big(\langle\Psi_n(x+1)|C^*_{x+1}|\mathrm{L}\rangle\langle\mathrm{L}| + \langle\Psi_n(x-1)|C^*_{x-1}|\mathrm{R}\rangle\langle\mathrm{R}|\big) \\
&\quad \times \left(|\mathrm{L}\rangle\langle\mathrm{L}|C_{x+1}|\Psi_n(x+1)\rangle + |\mathrm{R}\rangle\langle\mathrm{R}|C_{x-1}|\Psi_n(x-1)\rangle\right) \\
&= \|P_{x+1}\Psi_n(x+1)\|^2 + \|Q_{x-1}\Psi_n(x-1)\|^2.
\end{aligned} \tag{4.22}$$

Given that inner products $\langle \mathrm{L} \mid \mathrm{R}\rangle$ and $\langle \mathrm{R} \mid \mathrm{L}\rangle$ are zero (orthogonality of left and right states), this expression simplifies to:

$$\mu_{n+1}(x) = \|P_{x+1}\Psi_n(x+1)\|^2 + \|Q_{x-1}\Psi_n(x-1)\|^2. \tag{4.23}$$

By recognizing that $p_n(x+1)$ and $q_n(x-1)$ are defined as normalized squared norms of these projections (i.e., $p_n(x+1) = \frac{\|P_{x+1}\Psi_n(x+1)\|^2}{\mu_n(x+1)}$ and $q_n(x-1) = \frac{\|Q_x\Psi_n(x-1)\|^2}{\mu_n(x-1)}$), the lemma's equation is derived:

$$\mu_{n+1}(x) = p_n(x+1)\mu_n(x+1) + q_n(x-1)\mu_n(x-1). \tag{4.24}$$

This result highlights how the probability amplitude at a given position in a QW is determined by contributions from neighboring positions, consistent with the probabilistic nature of quantum state evolution.

Theorem 5, [26]. If initial distributions of both processes are identical, then their distributions remain identical at all subsequent times. distributions $\nu_n$ and $\mu_n$ of QWRW and QW will be identical at all steps $n$ if and only if their initial distributions $\nu_0$ and $\mu_0$ are the same.

$$\nu_0 = \mu_0 \Longleftrightarrow \nu_n = \mu_n \quad \text{for all } n \in \mathbb{N}_0. \tag{4.25}$$

Proof. By assuming that distributions $\nu_n$ and $\mu_n$ are equal at some arbitrary time $n$. Under this assumption, next step is to examine how these distributions evolve to next time step $n+1$. The evolution of distribution $\nu_{n+1}(x)$ is governed by a recurrence relation, which can be written as:

$$\nu_{n+1}(x) = p_n(x+1)\mu_n(x+1) + q_n(x-1)\mu_n(x-1), \tag{4.26}$$

where $p_n(x+1)$ and $q_n(x-1)$ are transition probabilities or coefficients that describe dynamics of the system at time $n$. This equation is derived from the assumption that $\nu_n = \mu_n$, thus substituting $\mu_n(x)$ into the equation for $\nu_{n+1}(x)$.

In Lemma 4, which likely establishes a relationship between distributions $\nu_{n+1}$ and $\mu_{n+1}$ under the given assumptions. By applying Lemma 4 to the recurrence relation, it follows that:

$$\nu_{n+1}(x) = \mu_{n+1}(x), \tag{4.27}$$

for all $x \in \mathbb{Z}$. This result demonstrates that if distributions are identical at some time $n$, then they will remain identical at next time step $n+1$. By induction, it follows that distributions $\nu_n$ and $\mu_n$ will be identical for all $n$ provided that they start from the same initial distribution, $\nu_0 = \mu_0$.

## 4.2 Simulation of Quantum Walk

In the context of a quantum RW, the coin operator $C_x$ is given by:

$$C_x = \frac{1}{\sqrt{2}} \begin{bmatrix} 1 & 1 \\ 1 & -1 \end{bmatrix}, \tag{4.28}$$

which is applied to the quantum state at each step. The initial state $\Psi_0(0)$ is defined as:

$$\Psi_0(0) = \frac{1}{\sqrt{2}} \begin{bmatrix} 1 \\ i \end{bmatrix}. \tag{4.29}$$

This initial state represents a superposition of two basis states with complex coefficients.

The coin matrix $C_x$ can be decomposed into projections $P_x$ and $Q_x$ which are associated with specific outcomes of the measurement:

$$P_x = |\mathrm{L}\rangle\langle\mathrm{L}|C_x = \frac{1}{\sqrt{2}} \begin{bmatrix} 1 & 1 \\ 0 & 0 \end{bmatrix} =: P, \tag{4.30}$$

$$Q_x = |\mathrm{R}\rangle\langle\mathrm{R}|C_x = \frac{1}{\sqrt{2}} \begin{bmatrix} 0 & 0 \\ 1 & -1 \end{bmatrix} =: Q. \tag{4.31}$$

Here, $P$ and $Q$ are projection matrices corresponding to left ($|\mathrm{L}\rangle$) and right ($|\mathrm{R}\rangle$) movement directions, respectively.

At $n = 0$, probabilities for finding the walker in respective positions are:

$$\nu_0(0) = \mu_0(0) = 1, \tag{4.32}$$

where $\mu_0(0)$ is the normalization constant. Given this, probabilities $p_0(0)$ and $q_0(0)$ of measuring the walker at position $x = 0$ after applying $P$ and $Q$ respectively are:

$$p_0(0) = \frac{\|P\Psi_0(0)\|^2}{\mu_0(0)} = \frac{1}{2}, \tag{4.33}$$

$$q_0(0) = \frac{\|Q\Psi_0(0)\|^2}{\mu_0(0)} = \frac{1}{2}. \tag{4.34}$$

To find existence probabilities at $n = 1$,

$$\nu_1(-1) = p_0(0)\nu_0(0) = \frac{1}{2}, \tag{4.35}$$

is used.

$$\nu_1(1) = q_0(0)\nu_0(0) = \frac{1}{2}. \tag{4.36}$$

Similarly, probabilities $p_1(\pm 1)$ and $q_1(\pm 1)$ are:

$$p_1(-1) = \frac{\|P\Psi_1(-1)\|^2}{\mu_1(-1)} = \frac{\|P^2\Psi_0(0)\|^2}{\|P\Psi_0(0)\|^2} = \frac{1}{2}, \tag{4.37}$$

$$q_1(-1) = \frac{\|Q\Psi_1(-1)\|^2}{\mu_1(-1)} = \frac{\|QP\Psi_0(0)\|^2}{\|P\Psi_0(0)\|^2} = \frac{1}{2}, \tag{4.38}$$

$$p_1(1) = \frac{\|P\Psi_1(1)\|^2}{\mu_1(1)} = \frac{\|PQ\Psi_0(0)\|^2}{\|Q\Psi_0(0)\|^2} = \frac{1}{2}, \tag{4.39}$$

$$q_1(1) = \frac{\|Q\Psi_1(1)\|^2}{\mu_1(1)} = \frac{\|Q^2\Psi_0(0)\|^2}{\|Q\Psi_0(0)\|^2} = \frac{1}{2}. \tag{4.40}$$

Thus, existence probabilities at $n = 2$ are:

$$\nu_2(-2) = p_1(-1)\nu_1(-1) = \frac{1}{4}, \tag{4.41}$$

$$\nu_2(0) = p_1(1)\nu_1(1) + q_1(-1)\nu_1(-1) = \frac{1}{2}, \tag{4.42}$$

$$\nu_2(2) = q_1(1)\nu_1(1) = \frac{1}{4}. \tag{4.43}$$

At $n = 3$, existence probabilities are:

$$\nu_3(-3) = \nu_3(3) = \frac{1}{8}, \tag{4.44}$$

$$\nu_3(-1) = \nu_3(1) = \frac{3}{8}. \tag{4.45}$$

The transition probabilities at $n = 3$ are:

$$p_3(-3) = q_3(-3) = p_3(3) = q_3(3) = \frac{1}{2}, \tag{4.46}$$

$$p_3(-1) = q_3(1) = \frac{5}{6}, \tag{4.47}$$

$$q_3(-1) = p_3(1) = \frac{1}{6}. \tag{4.48}$$

The evolution of these probabilities is the same as patterns observed in simple RWs initially but diverges since interactions between the coin and position operators come into play, [26]. For instance, at $n = 4$:

$$\nu_4(-4) = \nu_4(4) = \frac{1}{16}, \tag{4.49}$$

$$\nu_4(-2) = \nu_4(2) = \frac{3}{8}, \tag{4.50}$$

$$\nu_4(0) = \frac{1}{8}. \tag{4.51}$$

Other steps can be calculated similarly.

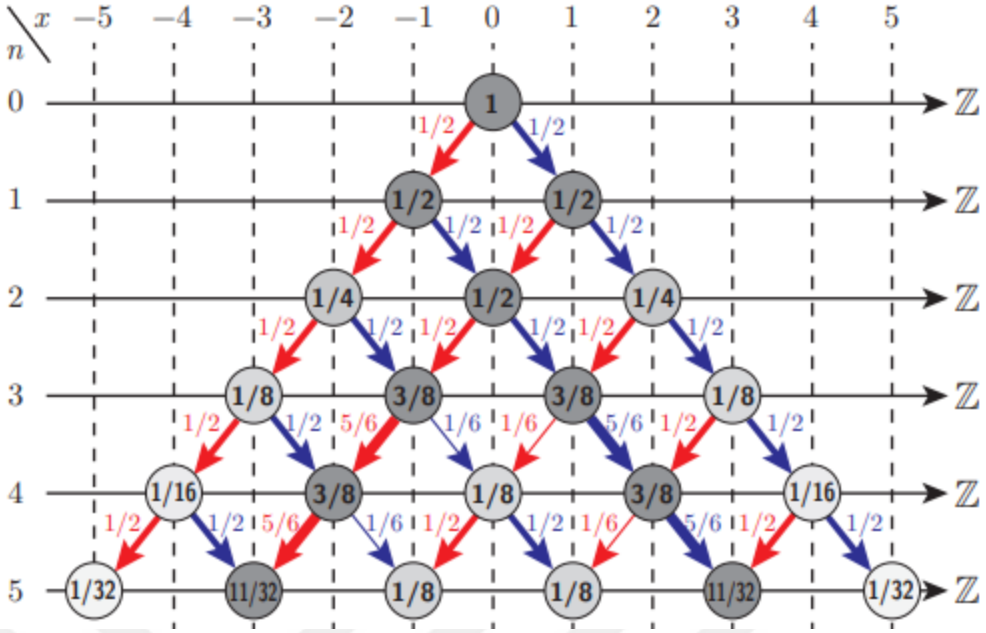



Figure 4.1: Left and right probabilities for 5 time step iterated QWRW, [26]

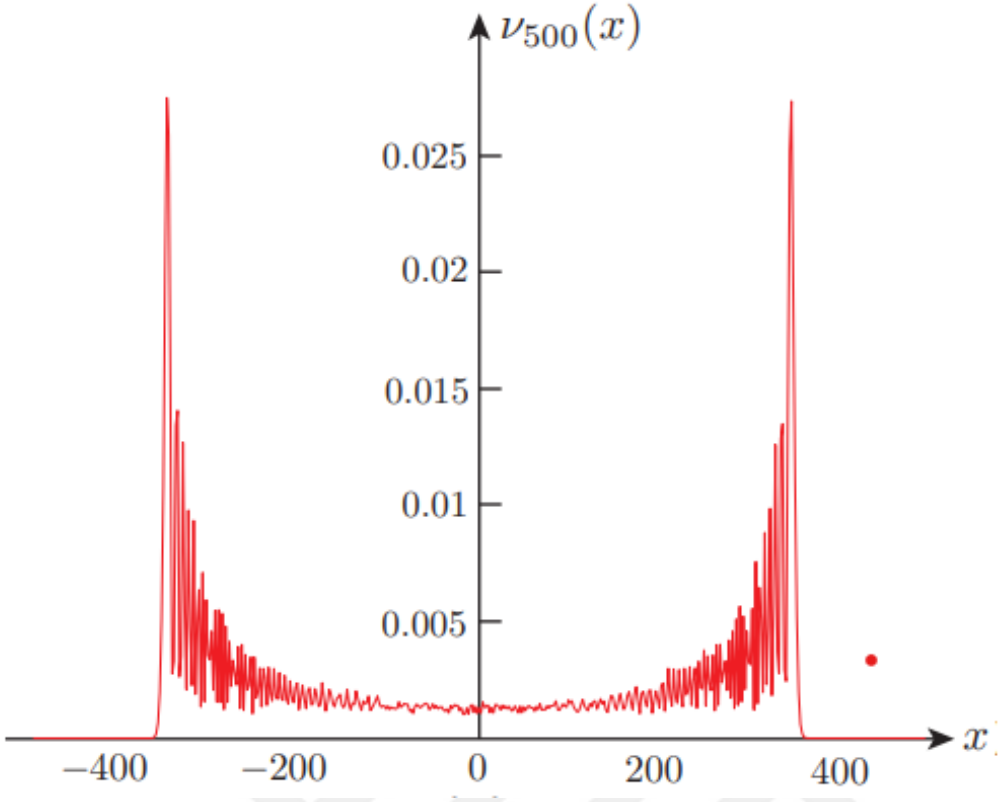



Figure 4.2: Probability distribution $\nu_n(x)$ of the QWRW at time $n = 500$, [26]

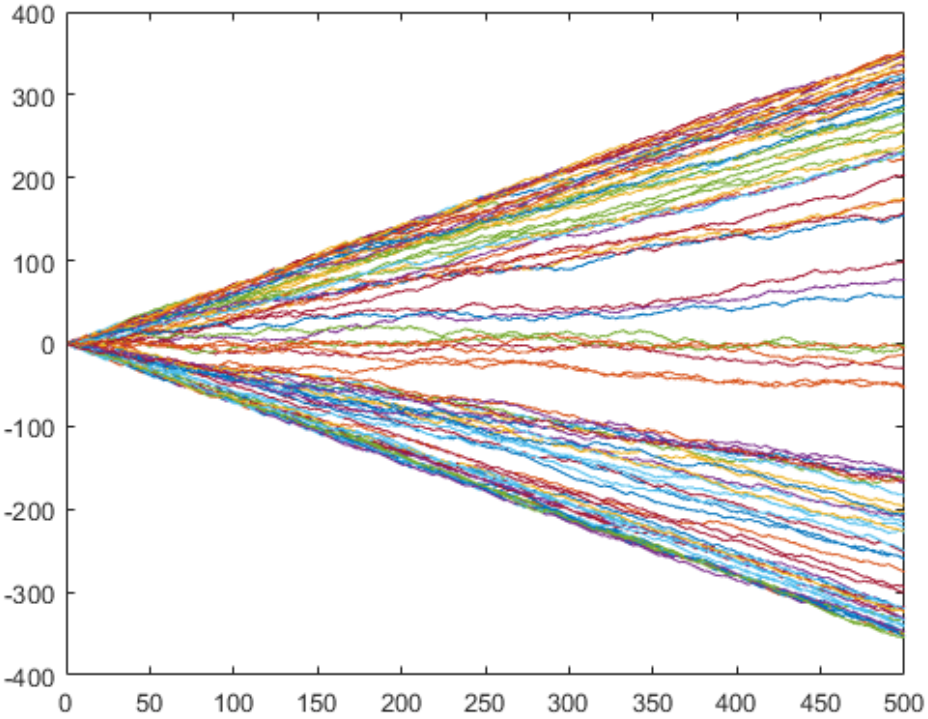



Figure 4.3: 100 simulated paths for $n = 500$, [26]

QWRW can be simulated using following MATLAB code:

```
function [liste] = qrw(Length,Size)
for z=1:Size
    L = Length;
P=[1/sqrt(2) 0; 1/sqrt(2) 0];
Q=[0 1/sqrt(2); 0   1/sqrt(2)];
psi= [ 0 0; 1/sqrt(2) complex(0,1)/sqrt(2); 0 0];
condprob=(norm(Q psi(:,2)) 2)/((norm(Q psi(:,2)) 2)+(norm(P psi(:,2)) 2));
ksi=2 binornd(1,condprob) 1;
sum=ksi;
j=2;
walk(1) = sum;
for n=2:L
    PS=zeros(2,n+2);
    PS(:,n+2)=[0 0];
    PS(:,1)=[0 0];

  for i=2:n+1
    PS(:,i)= P psi(:,i)+Q psi(:,i 1);
  end
  psi=PS;
  if ksi==1
      j = j +1;
  end
  condprob=(norm(Q psi(:,j)) 2)/((norm(Q psi(:,j)) 2)+(norm(P psi(:,j)) 2));
  ksi=2 binornd(1,condprob) 1;
  sum=sum+ksi;
  walk(n) = sum;
end
liste(:,z)= walk;
end
end
```

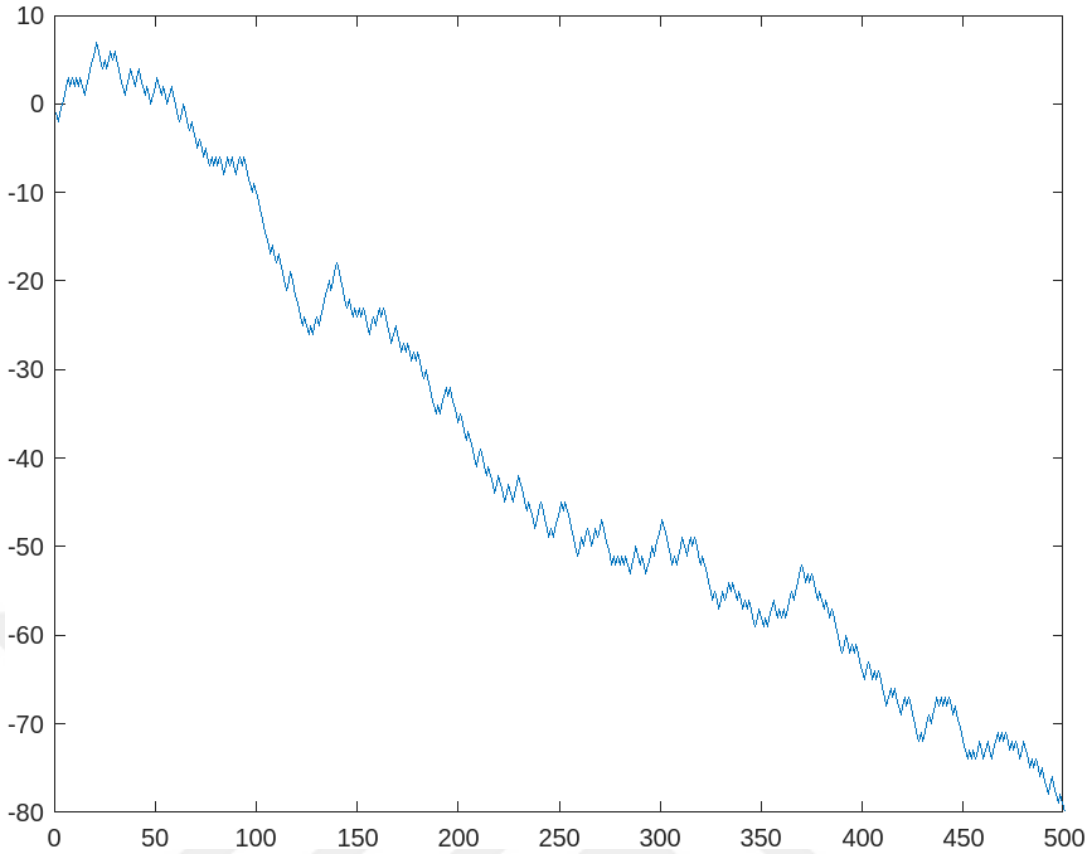



Figure 4.4: Sample path generated with provided MATLAB code for $n = 500$

# CHAPTER 5

## LONGEST HEAD RUN IN QUANTUM RANDOM WALK

This chapter primarily expands upon the concepts discussed in [23].

The length of the longest run of heads in a sequence of coin tosses, denoted as $R_n$, is a fundamental concept in probability theory, particularly in the study of random sequences. To analyze this, we define the cumulative distribution function $F_n(x) = \Pr(R_n \leqslant x)$, which gives the probability that the longest consecutive sequence of heads in $n$ tosses is less than or equal to $x$.

The function $F_n(x)$ is calculated in terms of the number of favorable outcomes, $A_n(x)$, which represents the number of sequences of length $n$ in which the longest run of heads does not exceed $x$. The probability is then given by normalizing the number of favorable outcomes by the total number of possible sequences of length $n$, which is $2^n$ for $n$ independent tosses of a fair coin. Formally, we express this relationship as:

$$F_n(x) = \frac{A_n(x)}{2^n} \tag{5.1}$$

where $2^n$ accounts for the total number of possible sequences, since each toss can result in either heads (H) or tails (T).

The computation of $A_n(x)$, which is the number of sequences of length $n$ where the longest run of heads does not exceed $x$, can be tackled through recursive partitioning of the set of favorable sequences. The partitioning is based on the number of heads (if any) that occur before the first tail appears. This method naturally leads to a recursive relationship because shorter sequences can be appended to form longer sequences without violating the condition that the longest run of heads is at most $x$.

For sequences of length $n \leqslant x$, any possible sequence of heads and tails is favorable

since, by definition, the longest possible run of heads in a sequence of length $n$ is $n$. In such cases, all sequences are allowed, and therefore:

$$A_n(x) = 2^n \quad \text{for} \quad n \leqslant x \tag{5.2}$$

This is because any sequence with $n \leqslant x$ will trivially satisfy the condition that the longest run of heads is no greater than $x$.

When $n > x$, we need to carefully structure the sequences to ensure that no sequence has more than $x$ consecutive heads. A key insight is that any sequence of length $n$ can begin with a specific pattern of heads followed by a tail, and the remaining sequence must adhere to the same constraint of having no more than $x$ consecutive heads. These initial patterns can be:

- The sequence starts with a tail (T),
- The sequence starts with one head followed by a tail (HT),
- The sequence starts with two heads followed by a tail (HHT),
- The sequence starts with three heads followed by a tail (HHHT), and so on.

Each of these patterns reduces the length of the remaining sequence and ensures that no part of the sequence contains more than $x$ consecutive heads. Thus, the recursive formula for $A_n(x)$ is:

$$A_n(x) = A_{n-1}(x) + A_{n-2}(x) + A_{n-3}(x) + \cdots + A_{n-x-1}(x) \quad \text{for} \quad n > x \tag{5.3}$$

This formula sums over all possible ways that a sequence of length $n$ can be constructed by appending a valid sequence of shorter length, where the longest run of heads does not exceed $x$.

To illustrate this recursive process, consider the case where $x = 3$. For sequences of length $n = 4, 5, 6, \ldots$, the recursive relation becomes:

$$A_n(3) = A_{n-1}(3) + A_{n-2}(3) + A_{n-3}(3) + A_{n-4}(3) \tag{5.4}$$

We start by computing the base cases:

$$A_0(3) = 1, \quad A_1(3) = 2, \quad A_2(3) = 4, \quad A_3(3) = 8 \tag{5.5}$$

These values correspond to all possible sequences of length $n \leqslant 3$, where any sequence is valid. Using the recursive relation, we compute further values for $n > 3$:

$$A_4(3) = A_3(3) + A_2(3) + A_1(3) + A_0(3) = 8 + 4 + 2 + 1 = 15 \tag{5.6}$$

$$A_5(3) = A_4(3) + A_3(3) + A_2(3) + A_1(3) = 15 + 8 + 4 + 2 = 29 \tag{5.7}$$

$$A_6(3) = A_5(3) + A_4(3) + A_3(3) + A_2(3) = 29 + 15 + 8 + 4 = 56 \tag{5.8}$$

This process continues, yielding values such as $A_8(3) = 208$. Hence, for $n = 8$, the probability that the longest run of heads does not exceed 3 is:

$$\Pr(R_8 \leqslant 3) = \frac{208}{2^8} = \frac{208}{256} = 0.8125 \tag{5.9}$$

This implies that for 8 tosses of a fair coin, there is an 81.25% chance that the longest run of heads will be no more than 3.

**In the case of a biased coin,** where the probability of heads is $p$ and the probability of tails is $q = 1 - p$, the problem becomes more complex. The number of favorable sequences, denoted $C_n^{(k)}(x)$, is the number of sequences of length $n$ with exactly $k$ heads, but where no run of heads exceeds $x$.

The probability that the longest run of heads is no greater than $x$ is then:

$$\Pr(R_n \leqslant x) = \sum_{k=0}^{n} C_n^{(k)}(x) p^k q^{n-k} \tag{5.10}$$

Here, the term $C_n^{(k)}(x)$ represents the number of sequences with exactly $k$ heads, constrained such that no run of heads exceeds $x$.

The values of $C_n^{(k)}(x)$ can be computed using a similar recursive structure to the one used for $A_n(x)$. For small values of $k \leq x$, $C_n^{(k)}(x)$ is simply given by the binomial coefficient $\binom{n}{k}$, since there are no constraints on the sequence. However, for larger values of $k > x$, $C_n^{(k)}(x)$ must account for the fact that no run of heads can exceed $x$. This leads to the recursive relation:

$$C_n^{(k)}(3) = C_{n-1}^{(k)}(3) + C_{n-2}^{(k-1)}(3) + C_{n-3}^{(k-2)}(3) + C_{n-4}^{(k-3)}(3) \tag{5.11}$$

This structure allows us to compute the probability for biased coins in a systematic manner. The key difference from the fair coin case lies in the weight given to each

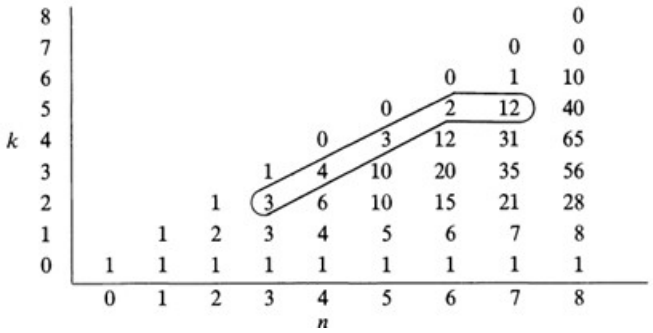



Figure 5.1: Values of $C_n^{(k)}(3)$ for $n \leq 8$

sequence, determined by the powers of $p$ and $q$ in the sum. Figure 5.1 shows the values of $C_n^{(k)}(3)$ for $n \leq 8$. The first four rows ($k = 0, 1, 2, 3$) correspond to Pascal's triangle. For the entries above these rows, they are determined by summing diagonally over four adjacent values from the rows and columns below and to the left. The 'hockey stick' pattern exemplifies the case $C_7^{(5)}(3) = 2 + 3 + 4 + 3 = 12$. The $A_n(3)$ values are the sums of the columns; for example, $A_8(3) = 1 + 8 + 28 + 56 + 65 + 40 + 10 = 208$. In the case of tossing a biased coin eight times, equation (3) gives the probability of obtaining no more than three consecutive heads as $1q^8 + 8pq^7 + 28p^2q^6 + 56p^3q^5 + 65p^4q^4 + 40p^5q^3 + 10p^6q^2$.

## 5.1 Quantum Walk Implementation

In the quantum walk case, calculating the probability of a particular outcome, such as the longest run of heads, becomes more intricate compared to the classical case. One key distinction arises from the non-commutative nature of the operators involved. Specifically, matrix multiplication in quantum systems is generally non-commutative, meaning that the product of two matrices $A$ and $B$ (i.e., $AB$) is not necessarily equal to $BA$. As a result, each path in the quantum walk must be evaluated individually, rather than relying on simplified algebraic structures like in classical random walks. This significantly increases the complexity of quantum walk calculations.

A useful approach in quantum walks may be to exploit the relationship between the probability of the longest run of heads being at most $x$ and its complementary event. Specifically, the probability that the longest run exceeds $x$, denoted as $\Pr(R_n > x)$,

can be used to compute $\Pr(R_n \leq x)$ through the equation:

$$\Pr(R_n \leqslant x) = 1 - \Pr(R_n > x) \tag{5.12}$$

This relationship allows for a reduction in the number of paths that need to be computed, as finding the probability that the longest run exceeds $x$ can be more tractable for certain values of $n$ and $x$.

To demonstrate this, consider the example where we calculate $\Pr(R_4 \leqslant 3)$ and $\Pr(R_5 \leqslant 3)$. Using the complementary relation, we first compute the probabilities that the longest run of heads exceeds 3 for $n = 4$ and $n = 5$.

For $n = 5$, the probability that the longest run exceeds 3, $\Pr(R_5 > 3)$, is given by:

$$\Pr(R_5 > 3) = \left\|(QP^4 + P^4Q + P^5)\Psi_0(0)\right\|^2 \tag{5.13}$$

Here, $P$ represents decomposed coin operator, which is responsible for advancing the walk left given in 4.3. $Q$ represents decomposed coin operator, which is responsible for advancing the walk right given in 4.3. $\Psi_0(0)$ is the initial quantum state of the walker. The terms $QP^4$, $P^4Q$, and $P^5$ account for the different possible paths that lead to a run of heads exceeding 3. These terms arise because, in quantum walks, paths can interfere, and thus each possible path must be considered separately.

Similarly, for $n = 4$, the probability that the longest run exceeds 3, $\Pr(R_4 > 3)$, simplifies to:

$$\Pr(R_4 > 3) = \left\|P^4\Psi_0(0)\right\|^2 \tag{5.14}$$

In this case, the quantum walker evolves according to the operator $P^4$, corresponding to four steps with the coin operator, and the result is applied to the initial state $\Psi_0(0)$.

The expressions for $\Pr(R_5 > 3)$ and $\Pr(R_4 > 3)$ are generalizable for any initial quantum state and coin matrix. In quantum walks, the initial state $\Psi_0(0)$ can vary depending on the specific setup of the quantum system. Additionally, the coin matrix, which dictates the probabilities of moving left or right in the walk, can be any unitary matrix, allowing for a wide variety of coin-flip dynamics.

In general, for any initial state $\Psi_0(0)$ and coin matrix $P$, the calculation of $\Pr(R_n > x)$ involves evaluating the norm of a series of quantum operators applied to the initial

state. The non-commutative nature of these operators requires that each possible path in the quantum walk should be considered individually, and the final probability is obtained by summing the contributions of each of these paths. The complementary relation $\Pr(R_n \leqslant x) = 1 - \Pr(R_n > x)$ may simplify the computation by focusing on the less complex event, $\Pr(R_n > x)$. However, note that as n gets large, that is considering the general case, such relations may not help with the calculations.

The longest head run quantum walk probabilities for further steps can be calculated through Monte Carlo;

```
function [longestheadprob, totallongestheads] = qrwlongestrunprob(Length, Size, threshold)
    longestheadcounts = zeros(Length + 1, 1);
    totallongestheads = 0;
     for z = 1:Size
        L = Length;
        P = [1/sqrt(2) 0; 1/sqrt(2) 0] ;
        Q = [0 1/sqrt(2); 0 1/sqrt(2)] ;
        psi = [0 0; 1/sqrt(2) complex(0,1)/sqrt(2); 0 0] ;
          condprob = (norm(Q psi(:,2)) 2) / ((norm(Q psi(:,2)) 2) + (norm(P psi(:,2)) 2));
        ksi = 2 binornd(1,condprob) 1;
        sum = ksi;
        j = 2;
        walk(1) = sum;
        headscount = 0;
        longestheads = 0;
         for n = 2:L
            PS = zeros(2,n+2);
            PS(:,n+2) = [0 0] ;
            PS(:,1) = [0 0] ;
            for i = 2:n+1
                PS(:,i) = P psi(:,i) + Q psi(:,i 1);
            end
            psi = PS;
            if ksi == 1
                headscount = headscount + 1;
                if headscount   longestheads
                    longestheads = headscount;
                end
            else
                headscount = 0;
            end
             condprob = (norm(Q psi(:,j)) 2) / ((norm(Q psi(:,j)) 2) + (norm(P psi(:,j)) 2));
            ksi = 2 binornd(1,condprob) 1;
            sum = sum + ksi;
            walk(n) = sum;
        end
        longestheadcounts(longestheads + 1) = longestheadcounts(longestheads + 1) + 1;
        if longestheads   threshold
            totallongestheads = totallongestheads + 1;
        end
    end
longestheadprob = longestheadcounts / Size;
end
```

# CHAPTER 6

# CONCLUSION

In this thesis, quantum walks have been examined as an extension of classical random walks, with a focus on the unique advantages driven by quantum phenomena such as superposition. Although quantum walks are often considered the quantum counterpart to classical random walks, they exhibit distinct features that do not occur in classical walks due to these quantum principles. These characteristics underscore the potential innovative applications of quantum walks in various fields.

Three different methods were presented and applied to analyze and understand the behaviors of quantum walks: analytical solution, computational solution, and trajectories.

- Analytical Solution: Analytical solutions were derived for quantum walks, allowing for a theoretical understanding of the walker's behavior over time. These solutions provided insights into probability distributions and the effects of quantum interference.
- Computational Solution: Numerical simulations of quantum walks were conducted using computational methods, enabling the exploration of scenarios that are difficult to solve analytically. This method played a critical role in uncovering the behaviors of quantum walks in more complex environments and validating theoretical predictions.
- Trajectories: The quantum-walk-replicating-random-walk (QWRW) approach was used to examine individual trajectories, offering a more classical interpretation of the walker's movement. This approach focused on step-by-step transitions, avoiding the complexities of quantum interference and providing new

insights into the directionality and behavior of quantum walks.

Through the combination of these methods, quantum walks were comprehensively analyzed, and their unique characteristics were thoroughly understood. While classical random walks served as a foundational concept, it was shown that the complexities and opportunities introduced by quantum walks, such as those enabled by superposition, are of great significance for both theoretical research and practical applications. The QWRW approach, in particular, opens opportunities for further exploration of trajectory-based analysis of quantum walks, potentially leading to new algorithms and insights in the field of quantum computing. Additionally, extending simulation methods to higher dimensions or different types of quantum walks could provide deeper understanding and new applications in this area.

# REFERENCES


[1] http://www.ibm.com/quantum-computing/learn/what-is-quantum-computing/. Accessed: 2021-09.

[2] Bassem Abd-El-Atty, Mohammed A. El-Affendi, Samia Allaoua Chelloug, and Ahmed A. Abd El-Latif. Double medical image cryptosystem based on quantum walk. *IEEE Access*, 11:69164–69176, 2023.

[3] Y. Aharonov, L. Davidovich, and N. Zagury. Quantum random walks. *Phys. Rev. A*, 48:1687–1690, Aug 1993.

[4] Michael Aizenman. The intersection of brownian paths as a case study of a renormalization group method for quantum field theory. *Communications in Mathematical Physics*, 97:91–110, 03 1985.

[5] Andris Ambainis, Eric Bach, Ashwin Nayak, Ashvin Vishwanath, and John Watrous. *One-dimensional quantum walks*, pages 37–49. STOC '01. Association for Computing Machinery, New York, NY, USA, 2001.

[6] Shankar Balasubramanian, Tongyang Li, and Aram Harrow. Exponential speedups for quantum walks in random hierarchical graphs. *arXiv*, 2307.15062, 2023.

[7] Arie Bar-Haim. Mapping a hadamard quantum walk to a unique case of a birth and death process. *arXiv*, 2104.04286, 2021.

[8] Alexei V. Chechkin, Ralf Metzler, Joseph Klafter, and Vsevolod Yu. Gonchar. *Introduction to the Theory of Lévy Flights*, chapter 5, pages 129–162. John Wiley and Sons, Ltd, 2008.

[9] Andrew M. Childs, Leonard J. Schulman, and Umesh V. Vazirani. *Quantum Algorithms for Hidden Nonlinear Structures*, pages 395–404. 2007.

[10] Richard P. Feynman, Robert B. Leighton, and Matthew Sands. *The Feynman lectures on physics / Vol. 3, Quantum mechanics*. Addison-Wesley, Reading, Mass., 1965.

[11] Irwin Huang and Yu-Ping Huang. Counteracting quantum decoherence with optimized disorder in discrete-time quantum walks. *Journal of Modern Optics*, 66(16):1652–1657, 2019.

[12] Abdo Abou Jaoudé. The paradigm of complex probability and the quantum entropic uncertainty principle. *The Paradigm of Complex Probability and Quantum Mechanics*, page 236–268, Feb. 2024.

[13] Karuna Kadian, Sunita Garhwal, and Ajay Kumar. Quantum walk and its application domains: A systematic review. *Computer Science Review*, 41:100–419, 2021.

[14] Yusuf Karlı. *Quantum Walks: Entanglement Between Spatial Degrees of Freedom and Interference in Multi-Photon Walks*. PhD thesis, iyte, 2020. Telif Hakkı - Database copyright ProQuest LLC; ProQuest does not claim copyright in the individual underlying works; Son güncelleme - 2024-06-28.

[15] David A. Kodde and Hein Schreuder. Forecasting corporate revenue and profit: Time-series models versus management and analysts. *Journal of Business Finance & Accounting*, 11(3):381–395, 1984.

[16] Wen Liang, Fei Yan, Abdullah M. Iliyasu, Ahmed S. Salama, and Kaoru Hirota. A hadamard walk model and its application in identification of important edges in complex networks. *Computer Communications*, 193:378–387, 2022.

[17] David A. Meyer. From quantum cellular automata to quantum lattice gases. *Journal of Statistical Physics*, 85(5–6):551–574, 1996.

[18] David Orrell. A quantum walk model of financial options. *Wilmott*, 2021(112):62–69, 2021.

[19] V. I. Pagurova, D. D. Sokolov, S. S. Marchenko, and et al. *Encyclopaedia of Mathematics: Volume 3: Heaps and Semi-Heaps — Moments, Method of (in Probability Theory)*, pages 723–950. Springer US, Boston, MA, 1995.

[20] Karl Pearson. The problem of the random walk. *Nature*, 72(1865):294–294, 1905.

[21] R. Portugal. *Quantum Walks and Search Algorithms*. Quantum Science and Technology. Springer New York, 2013.

[22] Eric Renshaw and Robin Henderson. The correlated random walk. *Journal of Applied Probability*, 18(2):403–414, 1981.

[23] Mark F. Schilling. The longest run of heads. *The College Mathematics Journal*, 21(3):196–207, 1990.

[24] Georgios D. Varsamis, Ioannis G. Karafyllidis, and Georgios Ch. Sirakoulis. Quantum walks in spaces with applied potentials. *The European Physical Journal Plus*, 138(4):312, 2023.

[25] Feng Xia, Jiaying Liu, Hansong Nie, Yonghao Fu, Liangtian Wan, and Xiangjie Kong. Random walks: A review of algorithms and applications. *IEEE Transactions on Emerging Topics in Computational Intelligence*, 4(2):95–107, 2019.

[26] Tomoki Yamagami, Etsuo Segawa, Nicolas Chauvet, André Röhm, Ryoichi Horisaki, and Makoto Naruse. Directivity of quantum walk via its random walk replica. *Complexity*, 2022(1):9021583, 2022.